Interactive comment on "Hypersensitivity of glacial temperatures in Siberia" by Pepijn Bakker et al.
Anonymous Referee #1

Bakker et al. look to understand the mechanisms responsible for Siberian climate at the LGM. To do so, they use a combination of PMIP2/3 simulations and CESM1 sensitivity tests. The authors find that the Siberian region has a large temperature and precipitation spread among models. Using their CESM1 sensitivity tests, Bakker et al. explore the sensitivity of the Siberian region to model physics, ice sheet configuration, and vegetation response. They find that the Siberian temperature response is most significantly influenced by the vegetation, especially when using CAM5, but ice sheet geometry and model physics are also important. Overall, this is a nice study that I believe will be a valuable contribution to understanding climate in a largely overlooked region at the LGM. However, I have a few questions about the model configurations and would like a bit more detailed exploration of mechanisms before publication.
We thank the reviewer for the kind words and for having a critical look at the manuscript.

Major Comments:
Additional information about the model setup is required. How was the original LGM simulation, from which these experiments were branched, configured? This is important, because as the authors find, the climate produced by CAM4 and CAM5 can be quite different. Therefore, despite branching from a previous run, I am not convinced that 200 years of spin up is sufficient. Including top-of-atmosphere energy imbalance would provide a first order estimate of how close these simulations are to equilibrium.
The LGM simulation from which we branched of was run with CAM5 and not including CN-dynamics (Carbon-Nitrogen-Dynamics). This simulation was run for a long time (>1000 years) and was very close to equilibrium, also shown by the TOA imbalance of -0.023Wm^{-2}. The relatively short, 200 year, LGM simulation with different model setup resulted in somewhat larger TOA imbalances for the simulations including CN-dynamics (-0.1Wm^{-2} for using CAM4 and -0.185Wm^{-2} using CAM5), however, we deem them sufficiently small, especially considering that the TOA imbalance for the corresponding PI simulations is of similar magnitude (-0.106Wm^{-2} for using CAM4 and -0.117Wm^{-2} using CAM5). The TOA imbalance resulting from the switch from CAM5 to CAM4 (without CN-dynamics) is negligible (0.014 for using CAM4 and -0.023Wm^{-2} using CAM5).

Also, are 30 year averages enough to produce true climatologies in this region? There are a lot of decadal oscillations that can impact climate for long periods (e.g. Deser et al. 2012). I don't think that this will significantly change results, but I do recommend a quick comparison with a longer average, such as 50 years, to make sure.
As suggested by the reviewer we compared 30 year and 50 year averages for a limited number of variables and simulations. Indeed the resulting changes in climatology are small, however the relative impact depends on the size of the signal that we are after. For the simulations with the largest LGM to PI JJA temperature difference in the Siberian target region (LGM_CAM5_Veg) the changes in LGM values resulting from the choice of averaging period (30 or 50 years) compared to the LGM to PI anomaly, are 2.1% for JJA surface air temperature and 2.5% for JJA precipitation, with absolute differences of 0.43K for temperature and 4.2mm/year for precipitation. For the simulations with the smallest LGM to PI JJA temperature difference in the Siberian target region (LGM_CAM4_noVeg) the impact of the choice of averaging period relative to the difference in LGM values are 21.5% and 8.3% for respectively JJA temperatures and precipitation in the Siberian target region.
We acknowledge the issue raised by the reviewer, but since we focus in the manuscript on the large inter-model differences, we deem the effect sufficiently small.

Finally, how were the CLM4 cases with "interactive vegetation" spun up? If not spun-up properly, it can take hundreds of years for the carbon cycle to come into equilibrium, which could impact your vegetation distribution.

The simulation with CN-dynamics were spun up using pre-industrial values. For the regions that have become land under LGM sea-level fall we used a nearest neighbor approach to obtain initial conditions. Indeed, especially the soil carbon pool takes centuries to equilibrate and therefore there are still trends in the different CN-pools. However, the trends in the local (Siberian) vegetation carbon pool, the most relevant for our analysis, is less than 2% of the total PI-to-LGM change in carbon pool over a 50-year period (both in CAM4 and CAM5). We deem this relatively small, but agree that a statement should be included in the manuscript to mention these trends. We added the following to the methodology section "Carbon pools in the litter and soils take centuries to equilibrate. However, we find that the trends are sufficiently small after 200 years to perform a robust analysis of the surface climate. Changes in Siberian (global) vegetation carbon pools are less than 2% (0.6%) of the total PI-to-LGM change) for the model years 150-200"

Limiting the analyses to JJA limits the mechanistic understanding. Are you sure that the summer changes are mainly a result of summer processes? Also, a more rigorous exploration of the local radiative effects versus heat transport would be useful. For example, albedo and cloud radiative forcings would be more insightful than snow and cloud cover.

Thank you for this interesting remark. We have performed an additional analysis looking at the seasonal cycle of PMIP multi-model variability for Siberian temperatures, cloud cover and snow cover. For all three variables it is clear that the large increase in differences between the various PMIP models going from PI to LGM is a summer feature. In the other seasons, temperature variance also increases somewhat, but cloud cover variance doesn't change while snow cover variance is in fact decreased.

In the updated manuscript we include these figures in the supplement as Figure A1 and mention them in the main text.

The authors argue for the necessity of additional CESM simulations based in part on the number of variables available for analysis from the PMIP simulations, but proceed to explore only basic outputs from their CESM experiments. Additional analyses to explore why the temperature changes in CESM with different configurations is warranted. At a minimum, areas of perennial snow cover are worth including. What about sea ice? Maybe a PDD and/or energy balance calculation would be insightful. With additional information, the authors could make a much more significant statement about which simulations would produce an ice sheet in Siberia at the LGM. From there, additional model assessment with proxies is possible. Are the models that produce a Siberian ice sheet too cold (probably) or too wet, etc. . .? What does this suggest about Siberian climate at the LGM?

We agree with the reviewer that many more interesting analyses could be performed using the set of CESM simulations. However, we want to stress that our main reason to include the CESM results is to be able to show which differences between PMIP simulations can potentially lead to large differences in Siberian JJA temperatures (ice sheets, atmopheric model and vegetation feedback). Such a separation of factors is not possible for the PMIP ensemble.

More CESM results for the different PI and LGM simulations are now provided in a new table (Table 3), including Siberian temperatures, minimum snow cover, cloud cover, precipitation and sea-level pressure.

Specific:

P1 Line 20: Further south than 50 ◦ N in many locations in North America.

We have changed the line to read "down to ~40 ◦ N in some areas.

P1 Line 21: Much of Alaska also did not have ice.
Indeed much of Alaska was also ice free during the LGM. We've changed the line to read "A notable exception was..."

P1 Line 25: Didn't some of these modeling studies limit their ice domain to exclude Siberia? Double check.
The work by Abe-Ouchi et al. (2013) was a free running modelling experiment that did not exclude Siberia from their domain (in fact they do simulate a Siberian ice sheet when applying an additional cooling factor). The other two studies are combined model-data driven reconstructions and as such they use the absence of an ice sheet in reconstructions as target in their modelling exercise.

P2 Line 2: Citation for the sea level statement?
We deem the notion that sea level was globally lower during the LGM as common knowledge and as such a reference is not needed here.

P2 Line 30: This dust feedback is mentioned in earlier (e.g. Mahowald et al., 1999; Ganopolski et al., 2010). What about the direct radiative effect of dust (e.g. Schneider et al., 2006)?
Thanks for pointing this out. We have added a reference to Mahowald et al. 1999 on line 27. We did not add it at line 30 as those are studies specifically discuss the evolution of the Siberian ice sheet in relation with LGM dust deposition. We prefer not to include a reference to Schneider et al. (2006) since they do not specifically discuss Siberia.

P4 Line 1: Link is messed up.
Thank you for pointing this out. I has been corrected.

P4 Line 10: Should be 1.9x2.5。
Thank you for pointing that out. We have adjust it.

P5 Line 16: Shouldn't this citation be for an ice sheet reconstruction paper? Peltier et al. (2015) maybe?
This reference has been updated to Ivanovic et al. (2016).

P5 Line 34: Not sure that ensemble is the correct word.
We have changed our wording. When referring to a small set of CESM experiments we call it a 'set of experiments', and only when we discuss all the CESM simulations combined do we now refer to it as an 'ensemble'.

P6 Line 5: Need to spell out LGM_CAM5_noVeg first.
Thank you for pointing this out. We have removed the acronym.

P6 Line 14: Why not look at the snow cover in the model?
We agree that this line is confusing and have therefor removed it. In the manuscript we do look at snow cover.

P6 Line 4: Cloud radiative forcing would be more insightful.
Cloud radiative forcing is unfortunately not available for all PMIP2 and PMIP3 LGM simulations.

P6 Line 13: Did you analyze CCSM3, as used in Liakka et al. (2016), to better understand this discrepancy? Could use a bit of additional discussion.

We do not think that there is a discrepancy per se. Possibly some of the models in the PMIP ensemble show results that resemble the one described by Liakka et al (2016). What we argue is that in the PMIP ensemble as a whole this mechanism does not seem to be the leading explanation for the temperature changes in Siberia. We have updated the main text accordingly.

Figure 1: Make the continental outlines thicker.
Figure has been updated

Figure 2: Darker green would make it easier to see.
Thank you for the suggestion. We improved the clarity of the figure by adding a magnified portion of the map highlighting the "target region".

Figure 3: Add winds and/or height anomalies to better highlight the circulation changes.
The contents of this figure have been changed from sea-level pressure to geopotential height anomalies at 500hPa to provide a much more direct indication of large-scale atmospheric circulation changes.

P10 Line 16: Why not plot the same variables as in the PMIP runs with CESM?
By showing geopotential height anomalies at 500hPa in figure 3 for the PMIP models and by adding summary information on CESM-based Siberian temperatures, minimum snow cover, cloud cover, precipitation and sea-level pressure in a new table (Table 3), we now effectively show the same variables for PMIP and CESM results as long as they are available.

P10 Line 22: How is surface roughness over the ice sheets configured? The results of Brady et al. (2013) suggest that this is important.
This is indeed one of those things that are uncertain for LGM simulations. We have chosen a simplified approach assigning a constant value similar to other areas that are ice covered at present day, but we agree that this is yet another mechanism that could impact temperatures since the sensitivity in the northeast Siberia to perturbations of the large-scale circulation is so large.

P10 Line 8-2?: It would be great to plot some of the differences mentioned.
We are not entirely sure what the reviewer is referring to in this comment, but assuming it is on the differences between CAM4 and CAM5, we would argue that such an analysis should really be performed by the experts who know all the details of the two atmospheric models.

P11 Line 20: How do you define vegetation density?
We use the term density here to describe in general how much vegetation there is per unit area, which in the model is mainly determined by the combination of the leaf area index and the stem area index.

P11 Line 22: This vegetation feedback has been found to be important for Arctic climate before (e.g. Jahn et al., 2005; Tabor et al., 2014).
Thanks for pointing this out. On page 11 we have added a line acknowledging this "Previous studies also found an important role of vegetation feedbacks in defining LGM Arctic temperatures (Jahn et al., 2005)."

Figure 5 A: There must be a strong local feedback in Siberia. Maybe plot snow cover or albedo?
Indeed there are multiple strong local feedbacks (snow cover, cloud cover changes etc). In a new table we have included information for the various CESM simulations on temperature, precipitation, cloud cover, snow cover and sea-level pressure in the Siberian target region.

Indeed temperature and the summer snow fraction are related, showing a local feedback. We added text to the main text describing some of the features of the data in this new table.

P11 Line 23: Does this mean the vegetation dies?

The different vegetation zones move southward, including the zone that has very little vegetation cover. In CESM the plant functional types are prescribed and thus not changing between the different experiments. They prescribe a mixture of different PFT's in every grid cell and the apparent southward shift of the vegetation zones is thus a change in the dominance of certain PFT's within the individual grid cells. We currently can't tell how the results would change if the PFT's would be interactively calculated using a full dynamic vegetation model.

P11 Line 26: Does Lawrence et al. (2011) discuss this Arctic LAI issue?

Thanks for pointing this out. Indeed Lawrence et al. (2011) also discuss that in CLM4 Siberian surface and soil temperatures are biased low (compared to observations) while CLM3 they were biased somewhat high. We added a short statement in the manuscript "….and is in line with the cold bias in modelled Siberian surface temperatures described by Lawrence et al. (2011)."

Figure 6: How were your PI runs configured for your LGM-PI anomalies? The vectors are very hard to see in panel C. Please change the color.

We do not understand the first part of this question. What is meant with configured in this context? We have made the vectors more clear.

Figure 7: Extend the temperature range in panel B.

Thanks for pointing this out. We have updated the figure to be more readable.

Interactive comment on "Hypersensitivity of glacial temperatures in Siberia" by Pepijn Bakker et al.
Anonymous Referee #2

Review of "Hypersensitivity of glacial temperatures in Siberia" by Bakker et al.
Geological evidence has shown that Siberia was partially glaciated during some glacial states while it kept mostly ice-free during others. Different previous studies have explored several potential explanations for these differences but a consensus is still lacking. Bakker et al. show that the ensemble of climate model experiments from PMIP2 and PMIP3 shows a very large spread in their simulated glacial summer (JJA) temperatures for the last glacial maximum (LGM) over Siberia. Bakker et al. argue that the large model spread could be an indication for a real "hypersensitivity" of glacial summer temperatures over Siberia, and hence regional glaciation itself. To explore some of the possible factors which may result in climatic differences over Siberia, they conduct several sensitivity simulations with CESM and show that the spread in simulations resulting from different ice sheet heights, vegetation feedback or changes in atmospheric physics of CAM4/5 can cause an equally large spread (∼20 K) as the PMIP model ensemble (∼24 K).

Overall, the manuscript is very well written and provides interesting insights into the problem of glacial summer temperature hypersensitivity and how it might explain the absence or presence of glaciation in Siberia during different glacials. However, the potential reasons for what may cause the large simulated temperature spread over Siberia could be explored in a bit more detail. I generally recommend publication in Climate of the Past after adding some more analysis to explain the summer temperature discrepancies.
We thank the reviewer for the kind words and for having a critical look at the manuscript.

General comments:
The study is very well written and presents very interesting and important aspects to better understand the possibly real "hypersensitivity" of the Siberian climate during glacials as well as the behaviour of models. Regarding the analysed variables in the manuscript, it is a bit difficult to understand whether local radiative processes (e.g. what about albedo, spring snow cover and lagged warming?) or large-scale temperature advection play a major role for the temperature spread – or both. Because Siberia builds up a spatially widespread thermal low during summer, the correlation between summer temperature and SLP can be expected to be mainly temperature driven. Increasing temperature will hence cause lower SLP which then can increase horizontal advection into Siberia. Consequently, changes in SLP would be rather a feedback to the warming (or cooling) and not the mechanism which causes the effect.
We agree with the reviewer that it is difficult to disentangle local versus large-scale effects on Siberian temperatures. This is especially true when doing so through the analysis of sea-level pressure fields. Fortunately we have found out that for all but one PMIP2/3 LGM simulation also geopotential height fields are available, and this makes for a more direct line of arguments and, in our opinion, a more convincing analysis to show that changes in the large-scale, circumarctic atmospheric circulation are indeed the cause of the spread in simulated Siberian JJA temperatures.
In the updated manuscript we show PMIP results for geopotential height anomalies at 500hPa (with the zonal mean removed), and together with the existing CESM geopotential height results we argue that both clearly show large-scale anomaly patterns that resemble a classical stationary wave pattern (wave number 2) and therefore indicate changes in the large-scale atmospheric circulation. Moreover, the four center of action in the PMIP based figure (figure 3) are the regions for which the relationship is significant, strengthening in our view the link with large-scale circulation as a driver. Based on CESM results we have already shown that as a result of these circulation changes, meridional heat transport into the region under discussion increases. This then reinforced the climatological thermal low in Siberia.

I also wonder whether the correlation in Fig. 3 is really statistically significant in terms of field significance given the low spatial degrees of freedom of SLP and that the relatively small regions with statistically significant correlations might be just those which are allowed to be significant by chance. In general, I would rather expect that the large-scale gradients in the pressure and temperature field e.g. relative to the Arctic and Tropics are important for temperature advection into Siberia. It would be interesting to see some analysis of the large-scale wind fields or pressure gradients and how different they are with respect to the model spread e.g. of the warmest vs. coldest PMIP member. I was also wondering if large-scale teleconnections might be very different for very warm vs. very cold simulations of Siberian summer temperatures (e.g. a one-point-correlation map of the averaged Siberian SLP and temperature with the northern hemisphere SLP and temperature).

We thank the reviewer for these interesting suggestions.

Likely as a consequence of the many differences within the PMIP ensemble, strong relationships such as the ones suggested by the reviewer have not been found. The strongest pattern we could find is a linear correlation between local (Siberian) JJA temperature anomalies and the large-scale stationary wave pattern anomalies (described by 500hPa geopotential height anomalies with the zonal means removed). The fact that this correlation map resembles a classical stationary wave pattern and that the four main centers of action are the regions for which the correlations are significant are to us strong indications of the importance of this mechanism to explain our findings. It is in this light that we would prefer to keep the significance levels in the figure. We have highlighted the latter points in the updated manuscript.

Regarding the large temperature spread over Eurasia, I was also wondering whether there is a potential link between warm and cold model experiments and the used atmospheric resolution (see below). In any case, the paper would strongly gain from a bit more detailed analysis and discussion of these aspects while the rest of the paper is very well written and does not require notable changes with exception of clarifying the sections about the role of the thermal low.

Specific comments:

Title of the paper: Maybe be more specific and write "glacial summer temperatures"?

Thanks for the suggestion. We have changed the title accordingly.

Page 2, line 2: Due to the quite shallow Arctic shelf, sea-level changes during the glacial lead to quite large changes in additionally exposed land during low level stands along the Arctic and Siberian coast. During summer, the additional landmass clearly increases the area which can heat up strongly during boreal summers with 24 hours of daylight. I could imagine that such an effect would be higher in models with a high horizontal resolution. It would be very interesting if you could add some information in the manuscript about individual ensemble members if there are indications that their differences in atmospheric resolution lead to systematic differences in Siberian temperatures.

In this context, there is one recent example where a very coarse resolution simulation has been repeated with the same ocean state and external forcing but using a 4x higher atmospheric resolution with CESM1 (Schenk et al. 2018) for the late glacial. In their supplementary figure 4, they show that a much higher atmospheric resolution with CESM1 predicts considerably warmer summers during the Younger Dryas stadial over Eurasia and Siberia compared to the coarse resolution simulation with CCSM3 despite using the same ocean state. They argue that atmospheric blocking in response to the Fennoscandian Ice Sheet (among other reasons) leads to warmer Eurasian summers. They show that the blocking and hence warmer summers are only captured at high resolution. Is this also the case for the warmest vs. coldest PMIP members?

Given the very strong difference in simulated summer temperatures at a different model resolution by Schenk et al. (2018) and the very important results of other studies concerning the atmospheric

flow disturbance by ice sheets (as already cited by the authors on page 3), I would suggest to add a paragraph about whether atmospheric resolution differences in the presence of large continental ice sheets can partly explain the spread of warming or cooling over Siberia.

The notion of a resolution dependency of the Siberian LGM temperatures is an interesting one. We have now added the PMIP-based LGM JJA temperature anomalies for the Siberian target region in table 1 to allow for such an analysis. When comparing these temperature anomalies with the spatial resolution of the atmospheric models (ranking both and plotting them against each other) we do not find any relationship. We have added a short comment to the concluding section of the manuscript to discuss the matter "Recently, Schenk et al. (2018) showed that the spatial resolution of the atmospheric model is key to obtaining realistic glacial temperature anomalies. However, we do not find any correlation between atmospheric model resolution and Siberian JJA LGM temperature anomalies (Table 1), despite having some models with a resolution very similar to one used by Schenk et al. (2018). We note, however, that we did not perform a dedicated experiment changing only the spatial resolution while keeping all other factors the same."

Regarding the exposed Arctic shelf during stadials: Is there any geological evidence that glaciations in Siberia might correlate with periods of higher sea-level stands (less exposed Arctic shelf and possibly cooler summers with a weaker thermal low and less advection)?

Perhaps MIS6 could represent such a geological period, but if such a correlation exists we dare not say based on the little data that we have.

Page 2, line 20: Can you give an example which one is good and possibly why?

This is not easy to do. First of all, some of these studies specifically included new mechanisms in order to obtain a good match (be it for the right reasons or not), and other studies show results of ice sheet models driven by multiple climate models and as a result they obtain very different configurations of the Siberian ice cover. For the introduction part of the current manuscript we don't think it is needed to go into the specifics of all these studies.

Page 5, line 1: Components of GLAC-1D have been published in different papers. Please add here the reference of the complete version which is Ivanovic et al. (2016).

Thank you for pointing this out. We have updated the text accordingly.

Page 5, line 3: Figure 5A is too small to see the important differences in ice sheet heights.

We agree that it is not easy from figure 5A to see the details of the differences in ice sheet height. An additional figure only showing these differences could be added to the supplementary material. However, we would like to stress that the details of the differences between these two LGM ice sheet reconstructions are not the focus of this study. In previous dedicated studies sensitivity experiments were performed in which they altered the height of the ice sheets, or even an individual ice sheet, in a controlled manner, or even removed one of the ice sheets completely. That allows for an in-depth study of its impact. When comparing the two ice sheet reconstructions used here we see that in some regions the one ice sheet reconstruction is higher, in other regions the other reconstruction, a complex picture (as shortly described in the method section) and as such one cannot easily make a connection with large-scale circulation changes. For the reader that is interested in the details of the two reconstructions we propose to add a reference to the work by Kageyama et al. (2017).

Page 5, line 27: The green contour line is not visible. Please add in addition the coordinates for the target region in the manuscript (for the analysed 1 ◦ x1 ◦ grid). Version

We improved the clarity of the figure by adding a magnified portion of the map highlighting the "target region". Giving the exact coordinates is not feasible since the region is not a

rectangle, but we have added a note about its approximate location "roughly located between 120E-180E and 70N-75N".

Page 6, lines 13-14: Regarding ". . .could be a consequence of local temperature changes. . .": This is quite certain as the low pressure over Siberia during summer is a thermal low and not a dynamic low. The sentence should be modified accordingly.

We agree with the reviewer that this section is not clear enough.

Indeed in this region warm summer temperatures lead to a low pressure system, a so-called thermal low. Previous work has suggested that local increases in sea-level pressure, driven by large-scale atmospheric circulation changes, lead to a decrease in cloud cover and a resulting increase in surface temperatures. The finding of a negative relationship in our study between local summer temperatures and sea-level pressure rather than a positive one, suggest that this mechanism can't explain the majority of PMIP results. Instead, in line with the formation of the thermal low mention by the reviewer, temperature changes lead to local changes in sea-level pressure.

To bring this message across to the reader this section now reads: "Moreover, a strong anticorrelation is found in the PMIP LGM simulations between JJA temperature and sea-level pressure anomalies over the Siberian target region (R=-0.72; p<0.05; Figure 2C): a more positive temperature anomaly locally creates a thermal low and hence corresponds to a lower sea-level pressure anomaly. Concurrently, higher sea-level pressure anomalies correspond to more positive cloud cover anomalies (R=0.50; p<0.05; Figure 2D). Liakka et al. (2016) found in their model that higher pressure is associated with lower cloud cover that in turn leads to an increase in JJA temperatures, but our results suggests that this is not the leading mechanism in the majority of PMIP LGM results."

Page 6, lines 15-16: The link to the Asian monsoon region and possibly other large-scale teleconnections are very important and should be explored a bit more in the manuscript.

We agree with the reviewer that these are interesting topics. However, we have found no indications that they are central to the description of the mechanisms driving the large inter-model differences in Siberian summer temperatures. As such we would like to keep the current focus of the manuscript.

Page 6, lines 17-25: The paragraph should be clarified with respect to the low being a thermal low. It appears odd to argue here that a deepening of the low-pressure cell over central Asia (it is not really a cell but rather a diffuse area) should control the amount of warming in Siberia when the deepening of the low is driven by the warming. This might be rather a positive feedback where warming increases convection which lowers the pressure which increases horizontal advection. This implies that another process causes the warming and the change in SLP is only a feedback. Please rewrite accordingly.

Using geopotential height anomaly maps (updated figure 3), we now show that local Siberian summer temperatures are linearly correlated with a change in the large-scale circumarctic stationary wave pattern. This provides indeed a much more direct link and therefor a discussion of the difficult to interpret 'far-field surface pressure anomalies' is no longer needed.

Page 10, lines 21-22: It would be interesting to get a number for the overall temperature change of the northern hemisphere in response to using a different ice sheet in CESM.

Thanks for pointing this out. We have now added a line "On a large scale, using the GLAC-1D ice-sheet reconstruction leads to a smaller LGM JJA temperature anomaly in the Northern Hemisphere (-6.4° C) than the simulation that includes the ICE-6G ice-sheet reconstruction (-7.2° C)."

Page 10, lines 24-25: This again is due to the thermal low which has to deepen with increasing temperature due to an increase in the rise of warm air.

Page 10, line 31: The similarity of the spatial anomaly pattern for temperature and SLP can be expected for the behaviour of the thermal low in summer. There has to be another reason for the warming first and the SLP change cannot be the mechanism but rather a positive feedback.

As mentioned above, we hope that the reviewer agrees that these issues are resolved by focusing on geopotential height anomalies rather than surface pressure anomalies.

Page 15, line 17: Please add a concluding paragraph about which model configuration for CESM (and e.g. which ice sheet) would be plausible for the LGM (no glaciation in Siberia) and why. In this context, can you give some examples about which PMIP models would be plausible for the LGM and absence of Siberian glaciation and which not and why?

We do not think this is feasible based on our analysis. The simulated temperature fields over Siberia (and as a result snow cover and potential ice sheet cover) are very different between models and more in line with geological data in some of them. We show that large changes in simulated temperatures can have many causes, from boundary conditions (ice sheets), to feedbacks (vegetation) to model formulation (atmospheric model). A 'good' simulation can thus result from various combinations of these factors. Moreover, there are indications that during previous glacial periods ice sheets existed in northeastern Siberia, so a 'good' model should also be able to simulate such a situation. We have added a short comment to the very end of the manuscript on the possible implications of our findings for the presence and absence of this ice sheet during various glacial periods "The combination of these factors, accompanied by local feedbacks can lead to strongly divergent summer temperatures in the region, which during some glacial periods could be sufficiently low to allow for the buildup of an ice sheet, while during other glacials, above-freezing summer temperatures will prevent a multi-year snow-pack, and hence an ice sheet, from forming. Finally, this high sensitivity of Siberian LGM summer temperatures in different climate models will present a major challenge in future modelling efforts using coupled ice-sheet-climate models."

Figure 1: The green contour in panel B is not visible.
Thanks for pointing this out. We have updated it.

Figure 2: Please strongly increase the size of numbers in the figure as well as the axis description.
Thanks for pointing this out. We have updated the axis description. However, the size of the numbers in the plots cannot be increased because they will start to overlap and make the figure more difficult to read.

Figure 3: Are the significant areas really statistically significant globally or only by chance? Given that the correlations may rather represent the thermal low, I'm not sure how this figure helps to understand the spatial spread over Siberia. Pressure gradients and teleconnections might be more suitable as they would represent how the changes of the thermal low interact with remote regions.
We agree that the correlations are not particularly strong. In the updated figure 3 we are now looking at the temperature relationship with the large-scale stationary wave pattern anomalies (described by 500hPa geopotential height anomalies with the zonal means removed), which provides a much more direct measure of the large-scale atmospheric circulation. The fact that this correlation map resembles stationary wave pattern and that the four main centers of action are the regions for which the correlations are significant, to us are strong indications of the importance of this mechanism to explain our findings. It is in this light that we would prefer to keep the significance levels in the figure. We have highlighted the latter points in the updated manuscript.

Figure 8: The red and blue for CAM4/5 is very difficult to see.

Thanks for pointing this out. We have updated it.

Table 1: It would be important to add a column here with the temperature difference LGM minus PI over Siberia for each model simulation to identify which models are unusually warm/cold. This would make it easy for others to further explore why which models differ from others. In this way, a potential dependency on the model resolution could be easily identified.
Thanks for pointing this out. We have included the information to table 1.

Table 2: Also here the temperature difference LGM minus PI over Siberia would be interesting.
Thanks for pointing this out. We have included the information to table 3.

Additional references:
Ivanovic, R. F. et al. Transient climate simulations of the deglaciation 21âĂŤ9 thousand years before present (version 1)âĂŤPMIP4 core experiment design and boundary conditions. Geosci. Model Dev. 9, 2563–2587 (2016).
Schenk, F. et al. Warm summers during the Younger Dryas cold reversal. Nature Commun. 9:1634 (2018).

Hypersensitivity of glacial summer temperatures in Siberia

Pepijn Bakker[1,2], Irina Rogozhina[3,2,4], Ute Merkel[2], and Matthias Prange[2]

[1]Department of Earth Sciences, Vrije Universiteit Amsterdam, Amsterdam, The Netherlands
[2]MARUM-Center for Marine Environmental Sciences, University of Bremen, Bremen, Germany
[3]Norwegian University of Science and Technology, Trondheim, Norway
[4]Institute of Physics of the Earth, Russian Academy of Science, Russia

Correspondence: Pepijn Bakker (p.bakker@vu.nl)

Abstract. Climate change in Siberia is currently receiving a lot of attention because large permafrost-covered areas could provide a strong positive feedback to global warming through the release of carbon that has been sequestered there on glacial-interglacial time scales. Geological evidence and climate model experiments show that the Siberian region also played an exceptional role during glacial periods. The region that is currently known for its harsh cold climate did not experience major glaciations during the last ice age, including its severest stages around the Last Glacial Maximum (LGM). On the contrary, it is thought that glacial summer temperatures were comparable to present-day. However, evidence of glaciation has been found for several older glacial periods.

We combine LGM experiments from the second and third phases of the Paleoclimate Modelling Intercomparison Project (PMIP2 and PMIP3) with sensitivity experiments using the Community Earth System Model (CESM). Together these climate model experiments reveal that the intermodel spread in LGM summer temperatures in Siberia is much larger than in any other region of the globe and suggest that temperatures in Siberia are highly susceptible to changes in the imposed glacial boundary conditions, the included feedbacks and processes, and to the model physics of the different components of the climate model. We find that changes in the circumpolar atmospheric stationary wave pattern and associated northward heat transport drive strong local snow and vegetation feedbacks and that this combination explains the susceptibility of LGM summer temperatures in Siberia. This suggests that a small difference between two glacial periods in terms of climate, ice buildup or their respective evolution towards maximum glacial conditions, can lead to strongly divergent summer temperatures in Siberia, allowing for the buildup of an ice sheet during some glacial periods, while during others, above-freezing summer temperatures preclude a multi-year snow-pack from forming.

1 Introduction

During the Last Glacial Maximum (LGM; ~24-18 ka) ice sheets covered large parts of the Northern Hemisphere continents. Over North America and northwestern Eurasia continental ice sheets extended from the Arctic ocean down to ~40°N in some areas. A notable exception was northeastern Siberia, a region that remained largely ice-free during the LGM according to archaeological evidence (Pitulko et al., 2004), geological reconstructions and permafrost records (Boucsein et al., 2002; Schirrmeister, 2002; Hubberten et al., 2004; Gualtieri et al., 2005; Stauch and Gualtieri, 2008; Wetterich et al., 2011; Jakobsson

et al., 2014; Ehlers et al., 2018), and combined model-data driven ice-sheet reconstructions (Abe-Ouchi et al., 2013; Kleman et al., 2013; Peltier et al., 2015). This is intriguing given the fact that the area presently extends as far north as ~75°N, and extended even further north during the LGM when a large part of the Siberian continental shelf was exposed because of eustatic sea-level lowering.

5   Reconstructing Quaternary ice sheet limits and assigning geological ages has for various reasons proven a difficult task for the Siberian region (e.g., Jakobsson et al., 2014). Svendsen et al. (2004) synthesized the existing geological data and concluded that since the penultimate glacial period (~140 ka), most of Arctic Siberia has remained ice-free, with the exception of the high-altitude Putorana Plateau and the coastal areas of the Kara Sea. Independent evidence from permafrost records (Boucsein et al., 2002; Schirrmeister, 2002; Hubberten et al., 2004; Wetterich et al., 2011), marine sediment cores (Darby et al., 2006;

10   Polyak et al., 2004, 2007, 2009; Adler et al., 2009; Backman et al., 2009) and dating of mollusc shells (Basilyan et al., 2010) also indicates that the entire region between the Taymyr Peninsula and the Chukchi Sea remained ice free and was covered by tundra-steppe during the LGM and that the last grounded ice impacts in different sectors of this region are dating back to MIS 6, or potentially MIS 5 within the dating uncertainties (Stauch and Gualtieri, 2008). Hence, the existing geological evidence indicates that ice sheets covered large parts of western Siberia (Svendsen et al., 2004; Patton et al., 2015; Ehlers et al., 2018)

15   and the East Siberian continental shelf (Niessen et al., 2013; Jakobsson et al., 2014, 2016) prior to the last glacial period but it remains unclear how often northeastern Siberia experienced large-scale glaciations during the different glacial periods of the Quaternary. Nonetheless, it appears that this far northern region was covered by ice during some glacial periods, while it remained ice free during others.

A number of studies have simulated the East Siberian LGM climate and ice sheet growth (e.g. Krinner et al., 2006; Charbit

20   et al., 2007; Ganopolski et al., 2010; Abe-Ouchi et al., 2013; Beghin et al., 2014; Peltier et al., 2015; Liakka et al., 2016). They show widely different results, from ice-free conditions to the buildup of a large ice sheet covering most of Siberia, and therefore the correspondence with proxy-based reconstructions ranges from good to very poor.

Over the years, a number of possible mechanisms have been suggested to explain the lack of an ice sheet covering eastern Siberia during the LGM, and perhaps therewith also explain the divergent results of coupled climate-ice-sheet simulations for

25   this region during the LGM. The most widely discussed mechanisms involve changes in atmospheric dust load, orographic precipitation effects and/or changes in atmospheric circulation driven by the buildup of the North American and/or Eurasian Ice Sheets.

During glacial times, the atmospheric dust load and dust deposition was likely substantially larger, particularly at the southern margins of the Northern Hemisphere ice sheets and over Siberia (Harrison et al., 2001; Lambert et al., 2015; Mahowald et al.,

30   1999, 2006). Modelling studies have shown that the buildup of ice over Siberia can be strongly impacted by the effect of dust on the surface albedo as an increase of dust deposition on the snow pack leads to a lowering of the snow albedo that in turn leads to higher melt rates (Krinner et al., 2006; Willeit and Ganopolski, 2018).

Continental ice sheets have a strong impact on the climate. It was already recognized by Sanberg and Oerlemans (1983) that under the influence of a preferred wind direction, an ice sheet can create a distinct asymmetry with high precipitation rates at

35   the windward side and low precipitation rates on the leeward side. This precipitation shadow effect has also been proposed

as an explanation for a westward migration of the Eurasian Ice Sheets during the last glacial period (Liakka et al., 2016, and references therein). Through the precipitation shadow effect, the buildup of the Eurasian Ice Sheet would lead to dry conditions in Siberia and potentially prevent the buildup of an ice sheet in the area.

Another way how ice sheets can impact the climate is through their steering effect on the large-scale atmospheric circulation. Broccoli and Manabe (1987) showed that the buildup of the North American ice sheets leads to substantial changes in the mid-tropospheric flow, including a split of the jet-stream around the northern and southern edges of the ice sheet and a resulting increase of summer temperatures over Alaska. Similar impacts of glacial ice sheets on large-scale atmospheric circulation were found in a number of other modelling studies (e.g. Cook and Held, 1988; Roe and Lindzen, 2001; Justino et al., 2006; Abe-Ouchi et al., 2007; Langen and Vinther, 2009; Liakka and Nilsson, 2010; Ullman et al., 2014; Liakka et al., 2016). Generally these studies indicate a warming over Alaska as a result of the growth of the North American ice sheets, but it differs from one study to the next how far westward this warming extends into Siberia. In these modelling studies the warming in Alaska and Siberia is linked to increased poleward heat transport induced by changes in the atmospheric stationary waves and to local feedbacks involving the surface albedo and atmospheric water vapor content (Liakka and Lofverstrom, 2018). A compilation of LGM temperature reconstructions based on various land proxy data provides support to these inferences, showing that LGM summer temperatures in Northern Siberia were overall not very different from the relatively mild present-day summer temperatures in the region (Meyer et al., 2017).

The lack of an LGM ice cover in northeastern Siberia has often been attributed to the increased atmospheric dust load and/or a precipitation shadow effect of the Eurasian Ice Sheet to the west. However, based on these mechanisms alone one cannot readily explain the absence of a Siberian ice sheet in some glacial periods, but its presence in others, or reconstructions of Siberian LGM summer temperatures close to present-day values (Meyer et al., 2017), suggesting that these processes are likely only part of the story. Existing and new coupled climate model results can shed light on these intriguing geological observations. Here we show that the inter-model spread of simulated LGM summer temperatures is exceptionally large in Siberia compared to any other region, suggesting a high susceptibility of Siberian summer temperatures to minor changes in boundary conditions or model formulation, and discuss potential underlying mechanisms and causes. We argue that this high susceptibility of Siberian summer temperatures to boundary conditions (hypersensitivity) is a major factor for the absence or presence of ice sheets in different Quaternary glacials.

2 Methodology

In this study we combine LGM simulations from the second and third phases of the Paleoclimate Modelling Intercomparison Project (PMIP2 and PMIP3) with LGM sensitivity experiments using the Community Earth System Model (CESM).

2.1 PMIP experiments

We use 17 LGM coupled climate model simulations from PMIP2 and PMIP3/CMIP5 (Table 1; Braconnot et al., 2007; Harrison et al., 2015) and their corresponding pre-industrial (PI) control simulations as a reference. LGM boundary conditions follow the

PMIP2 and PMIP3 protocols and include reduced greenhouse-gas concentrations, changed astronomical parameters, prescribed continental ice sheets and a lower global sea level. Nearly half (7/17) of these simulations include dynamic vegetation while the remainder uses prescribed PI vegetation (Table 1). See https://pmip2.lsce.ipsl.fr and https://pmip3.lsce.ipsl.fr for further details and references. The analysis of PMIP model output is based on climatological means and all output was regridded

5 to a common $0.9°\times1.25°$ horizontal resolution. In order to compare the sea-level pressure results from different models and between PI and LGM we removed the respective global mean before calculating the anomalies. For the analysis of geopotential height fields only 16 instead of 17 PMIP models are used because PMIP2 LGM geopotential height from ECHAM5-MPIOM was not available to us.

2.2 CESM experiments

10 To study the simulated LGM temperatures in the Siberian region in more detail and to isolate individual mechanisms, we analyzed a number of sensitivity experiments performed with the state-of-the-science coupled climate model CESM (version 1.2; Hurrell et al., 2013). The model includes the Community Atmosphere Model (CAM), Community Land Model (CLM4.0), the Parallel Ocean Program (POP2) and the Community Ice Code (CICE4). In all our CESM experiments, we use a horizontal resolution of $1.9°\times2.5°$ in the atmosphere (finite volume core) and land, and a nominal $1°$ resolution of the ocean (60 levels in

15 the vertical) and sea-ice models with a displaced North Pole.

For the CESM LGM simulations we followed the most recent PMIP protocol (PMIP4; Kageyama et al., 2017), including greenhouse-gas concentrations (190 ppm CO_2, 357 ppb CH_4 and 200 ppb N_2O), orbital parameters (eccentricity of 0.019, obliquity of $22.949°$ and perihelion-$180°$ of $114.42°$) and changes in the land-sea distribution and altitude due to lower sea-level (Di Nezio et al., 2016). In this study we used as default the GLAC-1D LGM ice sheet reconstruction (Ivanovic et al.,

20 2016). Note that the PMIP4 CH_4 concentration of 375 ppb is slightly higher than the one used here.

In the first set of sensitivity experiments we altered the imposed LGM ice sheet boundary conditions. Within the framework of PMIP4 two LGM ice sheet reconstructions are suggested as boundary conditions for the LGM experiments (Kageyama et al., 2017), namely GLAC-1D (Ivanovic et al., 2016) and ICE-6G (Peltier et al., 2015). When comparing these two ice sheet reconstructions we find substantial differences, especially an overall increase of the height of the North American ice sheets in

25 ICE-6G compared to GLAC-1D and a lowering of the Eurasian Ice Sheet (Figure 5A; both differences are on the order of 10% of the total ice sheet height, for more details see Kageyama et al., 2017). We performed a set of experiments to investigate the impact of these two different ice sheet reconstructions on simulated Siberian LGM temperatures (see "Continental ice sheets" set of experiments in table 2).

In the second set of sensitivity experiments, we used two different versions of the atmosphere model, CAM4 and CAM5, to

30 investigate the importance of the atmospheric model physics (see "Atmospheric model physics" set of experiments in table 2). CAM5 differs from its predecessor because it simulates indirect aerosol radiative effects by including full aerosol-cloud interactions. Furthermore, it includes improved schemes for moist turbulence, shallow convection and cloud micro- and macro-physics. Finally, while CAM4's grid has 26 vertical levels, in CAM5 four levels were added near the surface for a better representation of boundary layer processes. See Neale et. al. (2010) for a more detailed description of the atmospheric models

used in CESM.

Furthermore, the land model CLM4.0 includes the possibility to use a representation of the carbon-nitrogen cycle and to calculate the resulting changes in leaf area index, stem area index and vegetation heights per plant-functional-type (Lawrence et al., 2011). These changes in the biophysical properties of the vegetation cover impact, for instance, evapotranspiration and surface albedo. Note that the spatial distribution of plant-functional-types is prescribed in CLM4.0, which is why the model is sometimes described as a semi-dynamic vegetation model. Nonetheless, for simplicity we will refer to simulations that include carbon-nitrogen dynamics as 'interactive vegetation' simulations in the remainder of this manuscript. To study the interdependency of interactive vegetation and atmospheric model physics we performed a total of four experiments with either CAM4 or CAM5 and including or excluding interactive vegetation that are referred to as the "Interactive vegetation" set of experiments (Table 2).

All LGM experiments performed with CESM start from a previous LGM simulation and are run for at least 200 years to obtain a new surface climate equilibrium. Carbon pools in the litter and soils take centuries to equilibrate. However, we find that the trends are sufficiently small after 200 years to perform a robust analysis of the surface climate. Changes in Siberian (global) vegetation carbon pools amount to less than 2% (0.6%) of the total PI-to-LGM change for the model years 150-200. Climatologies are calculated based on the last 30 years of the simulations. For the sensitivity experiments focusing on interactive vegetation and atmospheric model physics, we also performed corresponding PI simulations (Table 2) to enable a proper analysis. Our five CESM LGM experiments are jointly referred to as the CESM LGM ensemble.

Throughout this manuscript we focus on boreal summer (June-July-August; JJA) near-surface air temperatures and simply referred to it as 'JJA temperatures' in the remainder of this manuscript. Moreover, when calculating LGM anomalies, we refer to the difference between an LGM simulation and the corresponding PMIP or CESM PI experiment (Table 2). It is in turn differences between these CESM LGM anomalies that we use to highlight mechanisms behind the susceptibility of Siberian summer temperatures (Section 3.2).

3   Results

3.1   Siberian LGM temperatures in PMIP2 and PMIP3 ensemble

The combined PMIP2 and PMIP3 LGM experiments reveal the particularity of LGM JJA temperatures in Siberia. Of all continental areas that were not covered by large ice sheets, Siberia shows the largest inter-model spread of LGM anomalies (standard deviation; Figure 1B). Another striking feature of the Siberian region is that it is one of the few regions where the PMIP multi-model mean temperature anomaly is close to, or even above zero in some areas, indicating that LGM summers were potentially as warm as at present (Figure 1A). Taken together, PMIP simulations show LGM JJA temperatures in Siberia ranging from warmer to substantially colder than at present. If we define a target region for Siberia based on the area where the PMIP multi-model spread is larger than 7°C (green contours in Figure 1; referred to as "Siberian target region" in the remainder of the manuscript and located roughly between 120°E-180°E and 70°N-75°N), we see that JJA temperature anomalies averaged over the target region for the individual models range between -12°C and +12°C (Figure 2 and Tabe 1). The spread in

5

simulated LGM temperatures in the Siberian target region increases compared to PI in all seasons, however JJA really stands out (top row figure A1).

Disentangling the causes of the particularity of the Siberian LGM summer temperatures based on PMIP results isn't straightforward because of multiple possible underlying causes; nonetheless, some aspects can be identified. Whereas the simulated temperature changes are quite different among PMIP models, a robust decrease in precipitation on the order of 20-30% is simulated (Figure 1C and 1D). As a consequence, the (Pearson) correlation between temperature change and precipitation change in the target region is insignificant at the 0.05 significance level (R=0.36; Figure 2A; note that throughout the manuscript, correlation refers to inter-model correlation). A significant correlation is found between temperature and snow cover, with higher temperatures corresponding to a lower snow cover (R=-0.60; p<0.05; Figure 2E). There are similarities between the spatial patterns of the PMIP multi-model spread in temperature anomalies and cloud cover anomalies (Figure 1B and 1F), however, within the Siberian target region local JJA temperature anomalies and cloud cover anomalies are not correlated at the 0.05 significance level (R=-0.45; Figure 2B), arguing against a leading role of local cloud dynamics to explain the large inter-model spread in Siberian temperatures. As in Yanase and Abe-Ouchi (2007), we find that a weakening of the North Pacific high during JJA is a consistent feature of PMIP LGM simulations (Figure 1G). Moreover, a strong anticorrelation is found in the PMIP LGM simulations between JJA temperature and sea-level pressure anomalies over the Siberian target region (R=-0.72; p<0.05; Figure 2C): a more positive temperature anomaly locally creates a thermal low and hence corresponds to a less pronounced sea-level pressure anomaly. Concurrently, higher sea-level pressure anomalies correspond to more positive cloud cover anomalies (R=0.50; p<0.05; Figure 2D). Liakka et al. (2016) found in their model that higher pressure is associated with lower cloud cover that in turn leads to an increase in JJA temperatures, but our results suggest that this is not the leading mechanism in the majority of PMIP LGM results. Inspecting the PI and LGM seasonal cycles for cloud and snow cover, we find that also for these variables the changes in inter-model spread in Siberia are most pronounced in summer. In contrast, the inter-model spread in precipitation doesn't change much between PI and LGM (Figure A1).

The strong negative correlation between JJA temperature and sea-level pressure anomalies suggests that the sea-level pressure changes could be a consequence of local temperature changes. Indeed, another reason for the negative correlation could be a remote forcing through anomalous heat advection into the Siberian target region. We find evidence for such a remote forcing of the temperature variations in the Siberian target region in the significant correlation with the large-scale mid-to-high latitude stationary wave pattern, resembling a wavenumber 2 structure (Figure 3). Increased Siberian JJA temperatures correspond with a lowering (increasing) of the JJA 500 hPa geopotential height to the southwest (southeast) of the region. The remote forcing of Siberian temperatures can thus be the result of an increase in northward flowing relatively warm air masses over the eastern part of the Asian continent into the region of interest.

A deeper understanding of the large multi-model spread in PMIP LGM JJA temperatures over Siberia and of the mechanisms proposed above is hampered by a multitude of differences between PMIP simulations: different model formulations, different parts of the climate system that are included and different boundary conditions including the uncertainty in the reconstructed LGM ice sheet and continental outlines. Moreover, certain key climate variables are not available for a sufficiently large number

of the PMIP models. In the following we will therefore investigate a purpose-built CESM-based ensemble of LGM simulations with clearly defined differences between the individual sets of sensitivity experiments.
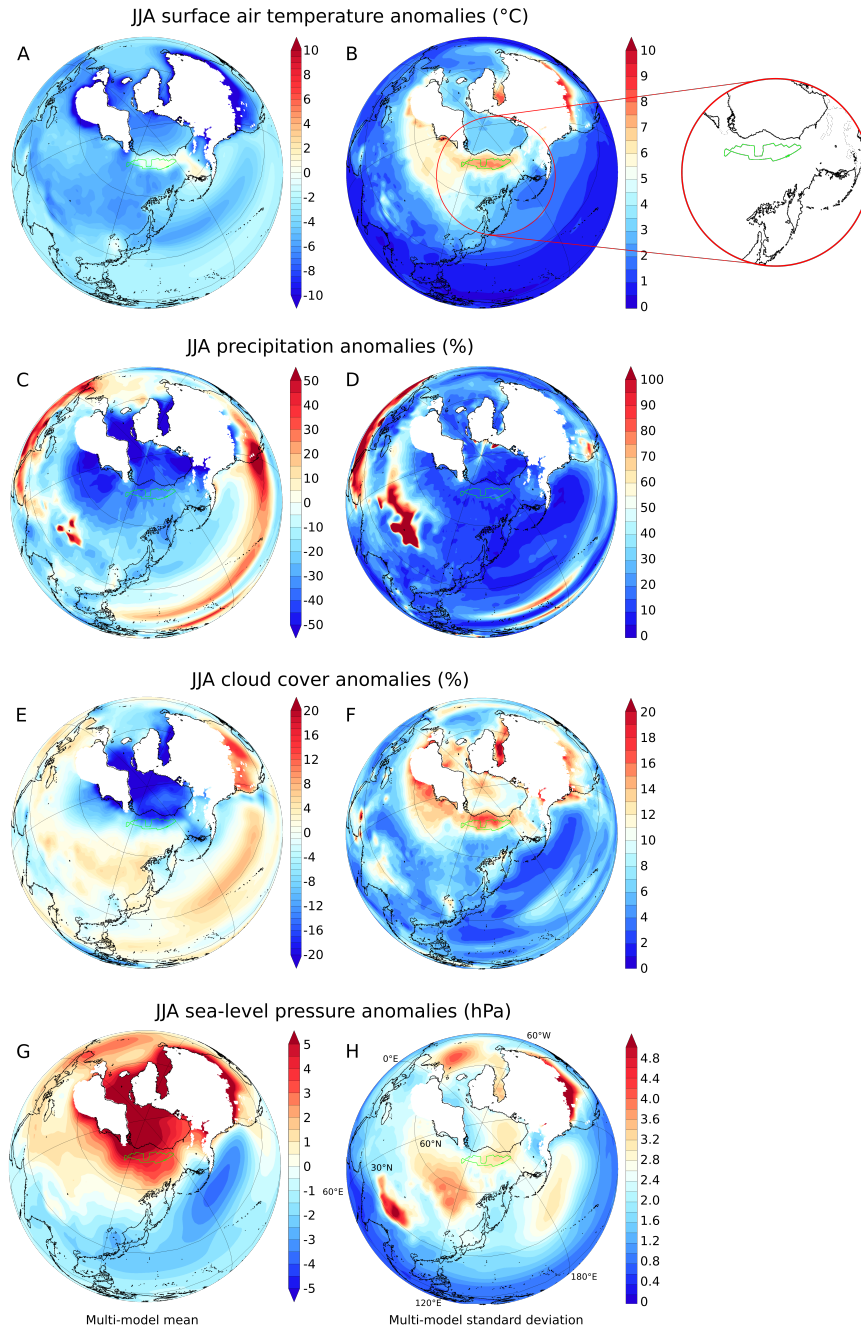
Figure 1. The PMIP2 and PMIP3 multi-model mean (left panels) and multi-model standard deviation (right panels) in LGM JJA climate anomalies. A-B: temperature anomalies (°C). C-D: precipitation anomalies (%). E-F: cloud cover anomalies (%); G-H: sea-level pressure anomalies (hPa). All anomalies are calculated with respect to PI. Note that regions covered by continental ice sheets during the LGM have been masked out. The green contour (shown in magnification in the top-right) shows the Siberian target region defined here as the region in which the PMIP multi-model standard deviation is larger than 7°C. The LGM coastlines are given in black.
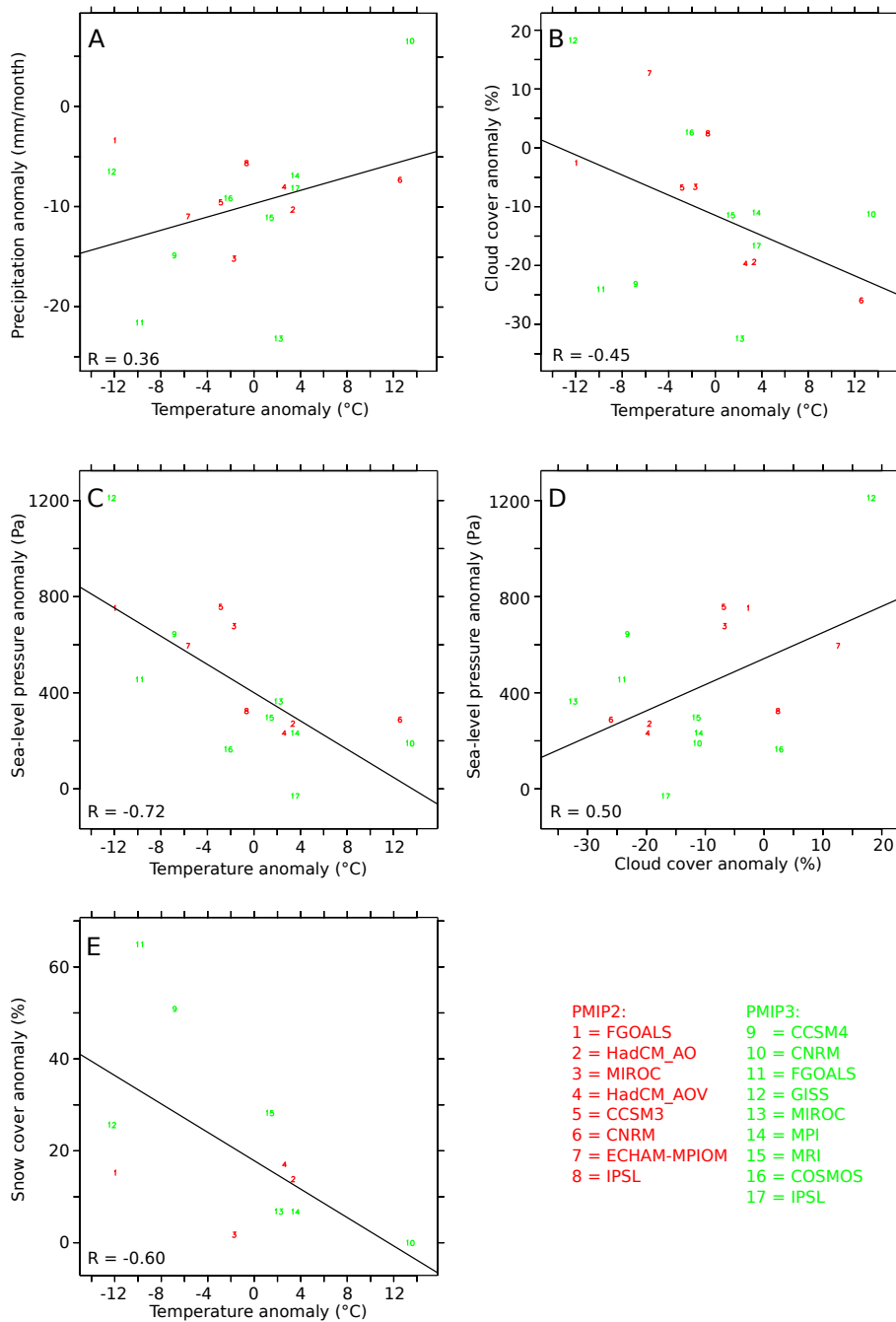
Figure 2. PMIP2 and PMIP3 LGM JJA climate anomalies averaged over the northeast Siberian target region. Red (green) numbers refer to the individual PMIP2 (PMIP3) experiments listed in the lower right. A: Precipitation anomalies ($\mathrm{mm\ month^{-1}}$) versus temperature anomalies (°C). B: Cloud cover anomalies (%) versus temperature anomalies (°C). C: Sea-level pressure anomalies (Pa) versus temperature anomalies (°C). D: Sea-level pressure anomalies (Pa) versus cloud cover anomalies (%). E: Snow cover anomalies (%) versus temperature anomalies (K). Black lines show linear fit and the R-value (Pearson correlation coefficient) as listed in the lower left corners of the different subfigures. R-values above 0.49 or below -0.49 indicate a significant correlation (p<0.05; t-test).

9
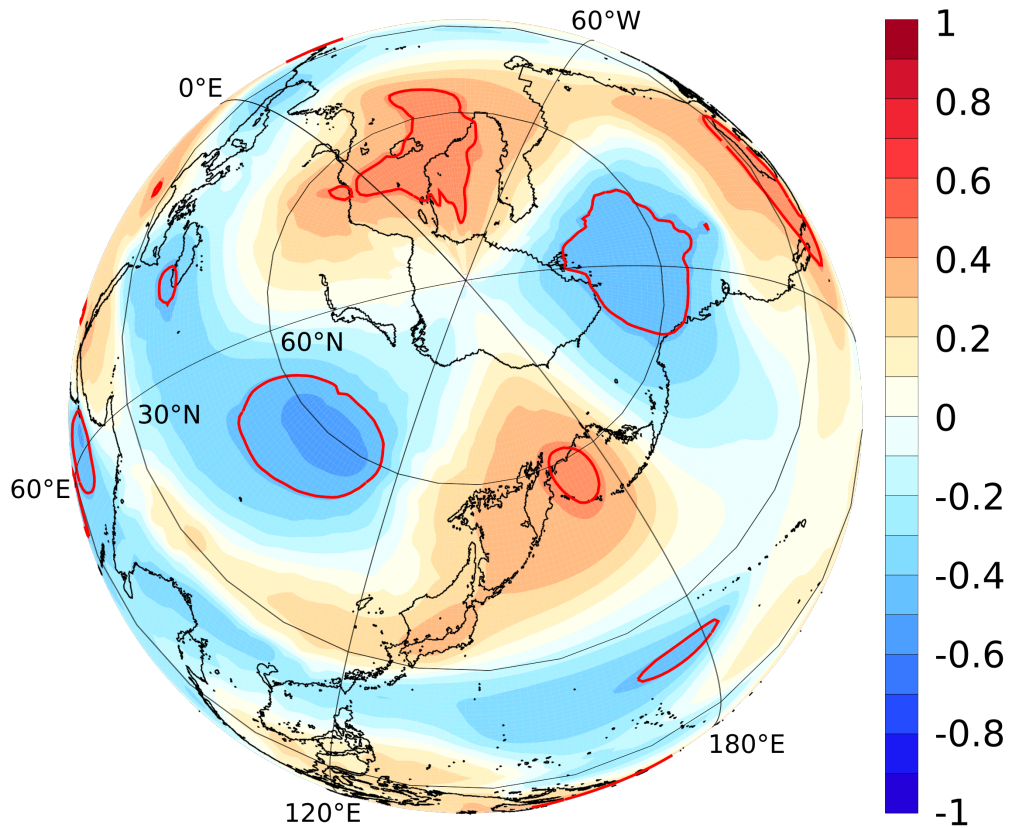
Figure 3. PMIP2 and PMIP3 linear correlations between JJA 500 hPa stationary wave geopotential height anomalies at any given location and JJA temperature anomalies averaged over the Siberian target region (see Figure 1 for the definition). Anomalies are calculated with respect to PI, and zonal mean geopotential height fields are subtracted before calculating the anomalies. The red contours bound the areas for which the correlation is significant ($p < 0.1$). The LGM coastlines are given in black.

3.2 Siberian LGM temperatures in CESM ensemble

We construct three sets of LGM sensitivity experiments performed with the CESM climate model in order to investigate in more detail the impact of changes in boundary conditions (continental ice sheets), model formulations (atmospheric model physics) and including different components of the climate system (interactive vegetation; Table 2).

5 Despite the fact that our total CESM LGM ensemble is smaller than the PMIP ensemble (n=5 instead of n=17) and that it wasn't designed to mimic the PMIP ensemble, we find that the spread in the CESM LGM temperature anomalies is surprisingly similar to the PMIP multi-model spread, both in terms of spatial distribution as well as magnitude (Figure 4B). This gives us confidence that investigating the causes of the sensitivity of northeastern Siberian temperatures in the CESM ensemble can provide insights into the PMIP inter-model differences. JJA temperatures in the Siberian target region for the individual CESM

10 experiments are listed in table 3.

First we analyze the first set of experiments ("Continental ice sheets"), differing only in the imposed ice sheet boundary conditions, namely LGM experiments forced by the GLAC-1D (LGM_CAM5_noVeg) or ICE-6G (LGM_CAM5_noVeg_ice6g) ice-sheet reconstructions (Table 2). On a large scale, using the GLAC-1D ice-sheet reconstruction leads to a smaller LGM JJA temperature anomaly in the Northern Hemisphere (-6.4°C) than the simulation that includes the ICE-6G ice-sheet reconstruc-

15 tion (-7.2°C; Figure 5A). Especially in the northeastern Siberian target region the LGM simulation using GLAC-1D ice sheets is substantially warmer (9.0°C) compared to the simulation using ICE-6G (6.0°C; Table 3). This can only be caused by changes in the large-scale atmospheric circulation since the simulations are identical apart from the ice sheets over North America and Eurasia. In line with the PMIP simulations, we find that higher JJA temperatures in the Siberian target region correspond to specific changes in the 500hPa geopotential height field, with negative anomalies to the southwest and positive anomalies to

20 the southeast (Figure 5B), and that this stationary wave pattern results in anomalous 500hPa southerly winds into the target region and a corresponding anomalous northward heat transport almost all the way from 30°N to the North Pole (Figure 5C). We thus find a high sensitivity of Siberian JJA temperatures with respect to relatively minor changes in the continental ice sheet geometries, which in turn induce changes in the circumpolar stationary wave pattern and anomalous northward heat transport in CESM. The similarity of the associated temperature and geopotential height anomaly patterns (wavenumber 2 structure;

25 Figure 5) with the PMIP-based response (Figures 1 and 3) suggests that this mechanism could also explain part of the spread in PMIP simulations. The anomalous northward heat transport we see in the stationary waves contributes to reinforce the (climatological) thermal low over Siberia and explains the negative relationship between JJA temperature and JJA surface pressure anomalies in the Siberian target region, both in the CESM "Continental ice sheets" set of experiments (Table 3) as well as in the PMIP results (Figure 2C).

30 The second set of CESM LGM simulations ("Atmospheric model physics"), is comprised of simulations in which different versions of the atmospheric model were used (CAM4 or CAM5; Table 2). Between the LGM_CAM4_noVeg and LGM_CAM5_noVeg simulations we find changes in the large-scale atmospheric circulation, in particular the stationary waves, and northward heat transport into Siberia (Figure 6) that are broadly similar to the response to different ice sheets as described above. Similar to the analysis of the PMIP models (Figure 3) and the CESM "Continental ice sheets" set of experiments (Figure 5), we find

that using different atmospheric model physics can lead to JJA warming (cooling) in the Siberian target region in response to enhanced (decreased) meridional heat transport into northeastern Siberia. Interestingly, if we look in more detail we find that the resulting surface temperature changes in Siberia are more complex in the "Atmospheric model physics" set of experiments than for the experiments described previously. There is warming in some parts of the region, but also cooling in other parts

5 (Figure 6A) and there are differences in the stationary wave pattern and in meridional heat transport. This is possibly related to slight shifts in the centers of action in the geopotential height anomalies and resulting changes in the airmasses that enter the Siberian target region. This highlights the complexity of comparing simulations with different atmospheric model versions that not only differ in their response of the large-scale atmospheric circulation to LGM boundary conditions, but also exhibit different local feedbacks with changes in cloud cover, humidity and pressure, which are directly influenced by, for instance,

10 differences in cloud parameterizations and radiative properties of the atmosphere. This point is further exemplified by the substantial differences between CAM4 and CAM5 in Siberian JJA temperatures and snow cover under PI conditions (Table 3). The models in the PMIP ensemble all differ in the included atmospheric physics and dynamics, thus the described mechansism in this CESM "Atmospheric model physics" set of experiments could as well explain (part of) the spread within the PMIP ensemble.

15 An important element in the high-latitude climate system is the vegetation-climate feedback. In the PMIP ensemble, 7 out of 17 models include the vegetation-climate feedback (Table 1). However, a systematic difference in simulated JJA LGM temperature anomalies for the Siberian region could not be found when comparing models with vegetation feedback with those that did not include this additional feedback. This doesn't come as a surprise if one considers the relatively small sample size with respect to all the inter-model differences that impact the simulated LGM JJA temperatures. We performed PI and LGM

20 simulations with CESM including and excluding interactive vegetation (the "Interactive vegetation" set; Table 2) to investigate its importance for Siberian temperatures. We find that the vegetation-climate feedback leads to a large LGM JJA cooling over Siberia, which is even more pronounced when using the CAM5 atmospheric model instead of CAM4 (Figure 7 and Table 3). If vegetation is allowed to respond to the changing climate through carbon-nitrogen dynamics, the tree and shrub limits shift south by several degrees of latitude as shown by the leaf area index (Figures 8A and 8C). In CESM, the presence of vegetation,

25 its height as well as its density have a large impact on the surface albedo through the vegetation-albedo feedback: vegetation that protrudes through the snow pack lowers the surface albedo that in turn leads to a positive feedback loop with increasing temperatures, more snow melt, more vegetation growth and an even lower surface albedo. Accordingly, the situation in the CESM simulations including interactive vegetation is such that the cold and snow covered landscape limits vegetation growth and leads to a southward migration of the tree and shrub limits. This relationship between vegetation and snow cover also

30 determines the resulting LGM JJA temperature changes (compare figures 7A and 8C; Table 3). Previous studies also found an important role of vegetation feedbacks in defining LGM Arctic temperatures (Jahn et al., 2005). The impact of interactive vegetation in CESM is also clearly seen in the PI simulations, resulting in a substantial decrease in the leaf area index with respect to the prescribed values (Figure 8A and 8B) and is in line with the cold bias in modelled Siberian surface temperatures described by Lawrence et al. (2011) (see also table 3).

35 Looking at all the experiments in the third set of experiments ("Interactive vegetation", table 2), using different atmospheric

model physics (Figure 6) with or without interactive vegetation (Figure 7), we find that the strong cooling in Siberia in the simulation that combines both the different atmospheric model physics and interactive vegetation (LGM_CAM5_Veg; Figure 7B), is not readily explained as a linear combination of the two individual effects. This is true for Siberian JJA temperatures, but also for other key climate variables (Table 3). It should be noted that the simulations with the lowest JJA LGM temperatures in table 3 are in fact the ones with the highest precipitation rates (not only in JJA, but also in the annual mean; not shown). This all shows the complexity of the response to a combination of factors, in this case changes in large-scale atmospheric circulation, local atmospheric processes and local land-surface processes. It is to be expected that the response of individual PMIP simulations is similarly complex.

5

JJA surface air temperature anomalies (°C)

CESM ensemble mean

CESM ensemble standard deviation
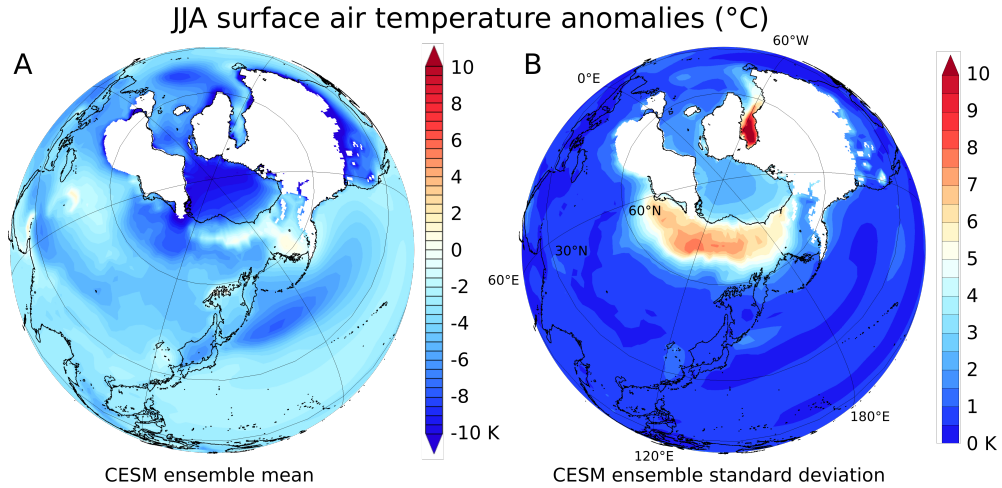
Figure 4. CESM ensemble mean (A) and ensemble standard deviation (B) of LGM JJA temperature anomalies (°C). Note that regions covered by continental ice sheet during the LGM have been masked out. The LGM coastlines are given in black.

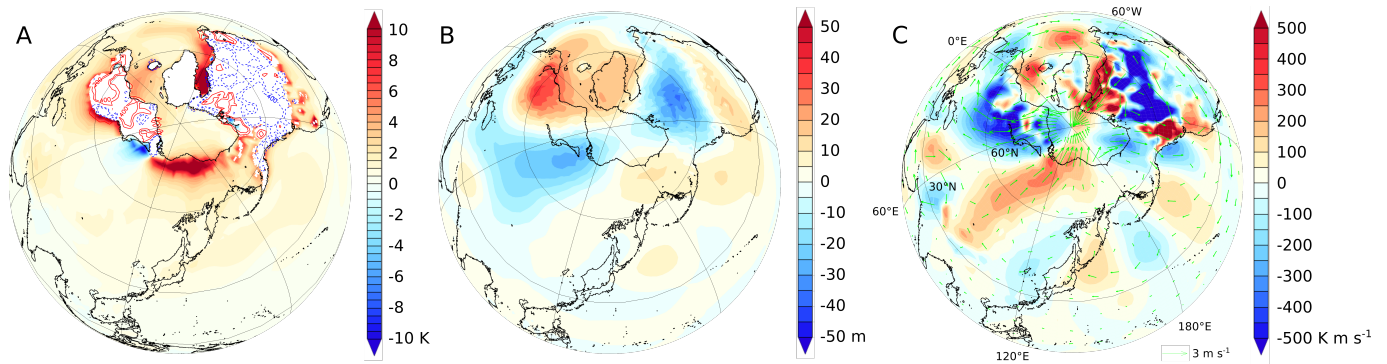**Figure 5.** Impact of the prescribed LGM ice-sheet topography (GLAC-1D versus ICE-6G) on simulated LGM climate anomalies during the boreal summer season (JJA). Results are shown as the CESM experiment LGM_CAM5_noVeg minus LGM_CAM5_noVeg_ice6g. A: near-surface temperature anomalies (K). B: 500hPa geopotential height anomalies (m; anomalies calculated after subtracting the zonal mean). C: vertically averaged meridional sensible heat transport anomalies (Kms^{-1}; shading). Vectors in panel C show 500 hPa wind anomalies (ms^{-1}). In panel A regions covered by continental ice sheets during the LGM have been masked out. The red (blue) contours in panel A depict positive (negative) differences in ice sheet height (m) between the GLAC-1D and ICE-6G reconstructions (GLAC-1D - ICE-6G; 300 m contour interval). The LGM coastlines are given in black.
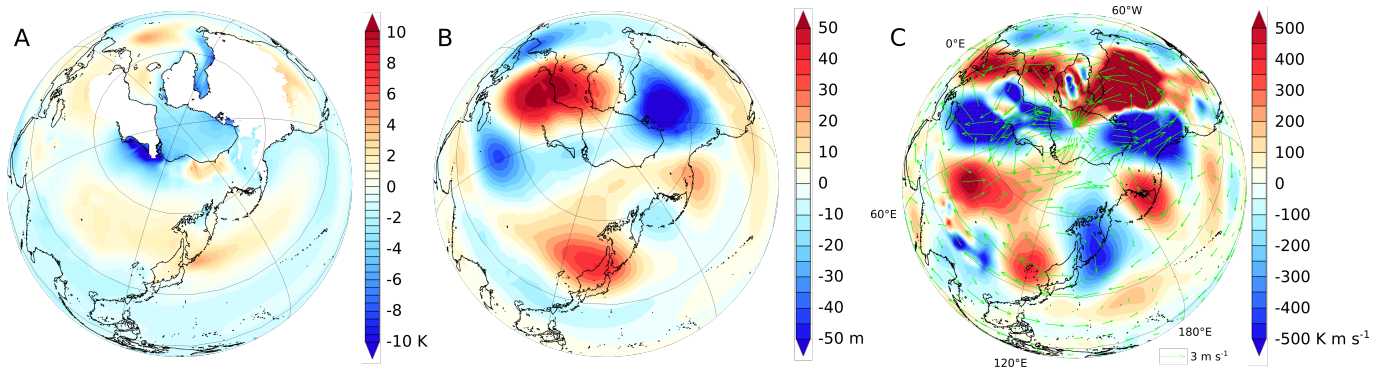
Figure 6. Impact of using different atmospheric models (CAM5 versus CAM4) on simulated LGM climate anomalies during the boreal summer season (JJA). Results are shown as LGM-PI anomalies for LGM_CAM5_noVeg minus LGM_CAM4_noVeg. A: near-surface temperature anomalies (K). B: 500 hPa stationary wave geopotential height anomalies (m; anomalies calculated after subtracting the zonal mean). C: vertically averaged meridional sensible heat transport anomalies (Kms^{-1}; shading). Vectors in panel C show 500 hPa wind anomalies (ms^{-1}). In panel A regions covered by continental ice sheets during the LGM have been masked out. The LGM coastlines are given in black.
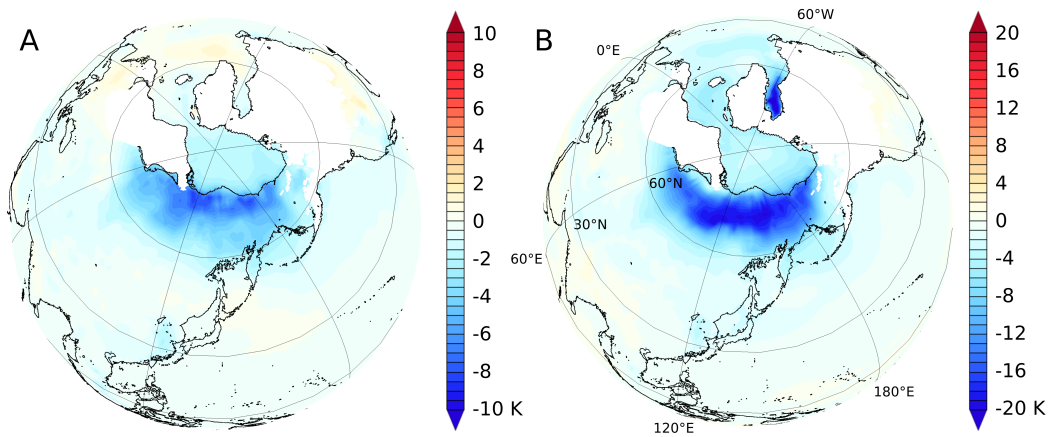
Figure 7. JJA LGM temperature anomalies showing the impact of introducing vegetation-climate feedbacks. Results are shown as LGM-PI anomalies for CAM4 (A; LGM_CAM4_Veg – LGM_CAM4_noVeg) and CAM5 (B; LGM_CAM5_Veg – LGM_CAM5_noVeg). Regions covered by continental ice sheets during the LGM have been masked out. The LGM coastlines are given in black. Note the different scaling used for the two panels.
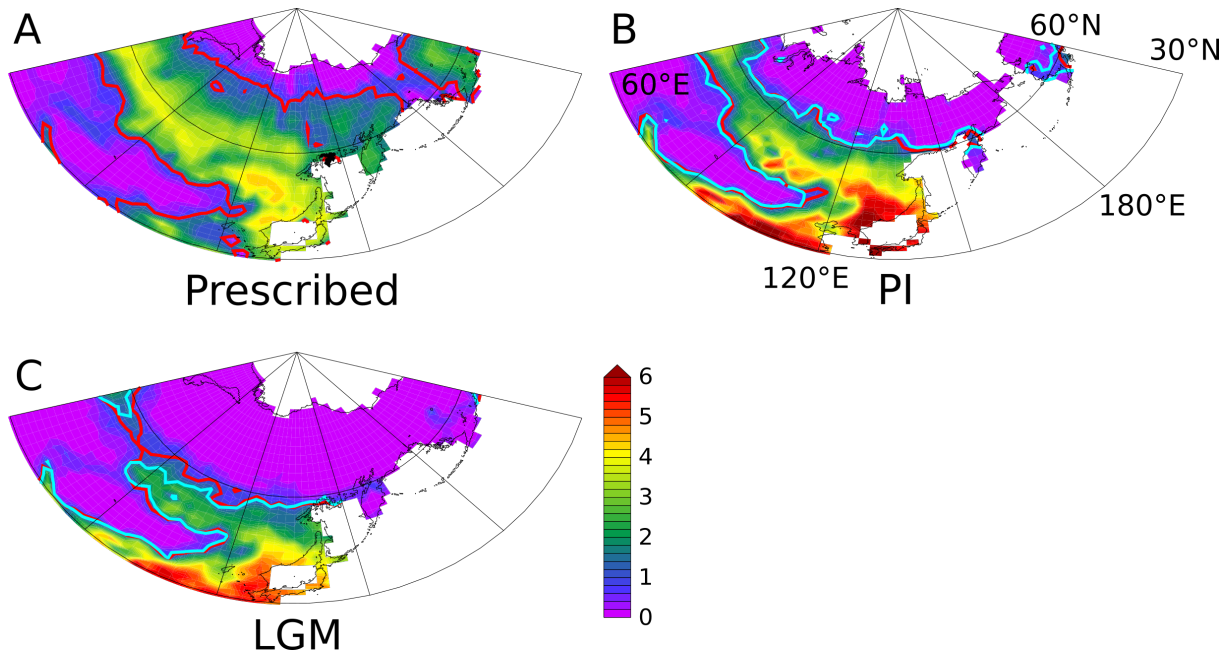
15

Figure 8. Leaf area index ($m^2 m^{-2}$) in northeastern Asia as prescribed in the simulations without interactive vegetation (A), and as simulated in the pre-industrial (B) and LGM (C) CAM4_Veg experiments including interactive vegetation. Contours give the leaf area index of 1 $m^2 m^{-2}$ (red for CAM4 and light blue for CAM5).

4   Concluding remarks

From a climate model perspective, LGM JJA temperatures in northeastern Siberia appear highly susceptible to changes in the imposed boundary conditions, included feedbacks and processes, and to the model physics of the different climate model components; much more so for Siberia than for any other region. This becomes apparent from the comparison of 17 different

5   PMIP2 and PMIP3 LGM experiments, as well as from three sets of CESM sensitivity experiments. The spread in Siberian JJA LGM temperature anomalies in the CESM ensemble is ~20°C, which is comparable to the inter-model spread of ~24°C found in the PMIP simulations. The main cause appears to be that relatively small changes in the continental ice sheets or model physics can lead to large changes in meridional atmospheric heat transport related to changes in the circumpolar atmospheric stationary wave pattern, in line with Ullman et al. (2014) and Liakka and Lofverstrom (2018). Local snow-albedo

10 and vegetation-climate feedbacks strongly amplify the Siberian JJA temperature change. Recently, Schenk et al. (2018) showed that the spatial resolution of the atmospheric model is key to obtaining realistic glacial temperature anomalies. However, we do not find any correlation between atmospheric model resolution and Siberian JJA LGM temperature anomalies (Table 1), despite having some models with a resolution very similar to the one used by Schenk et al. (2018). We note, however, that we did not perform a dedicated sensitivity experiment changing only the spatial resolution while keeping all other factors the

15 same.

In most of the examined PMIP LGM simulations Siberia receives less precipitation; however, we don't find indications that the buildup of a Siberian ice sheet was hampered by the absence of precipitation. On the contrary, in both the PMIP ensemble as our CESM experiments we find that local precipitation and JJA temperature changes are not significantly correlated, while cooler summers are strongly correlated to a higher snow cover, suggesting that a cold climate would be associated with a perennial

5   snow cover. Neither do we find support for the notion that changes in large-scale atmospheric stationary wave patterns drive Siberian JJA temperatures directly through local cloud changes.

Although situated at high northern latitudes, geological evidence suggests that Siberia was covered by continental ice sheets during some glacial periods, but remained largely ice free during others, for instance the last glacial period including the LGM. Increased atmospheric dust deposition and a precipitation-shadow cast by the Eurasian Ice Sheets to the west are often listed as

10   possible causes; however, such mechanisms cannot readily explain the absence of a Siberian ice sheet in some glacial periods, but its presence in others, or conform with the independent reconstructions of Siberian LGM summer temperatures close to present-day values (Meyer et al., 2017). This is suggesting that these processes are likely only part of the story, and here we argue for the importance of changes in meridional atmospheric heat transport and the configuration of the northern hemisphere continental ice sheets in order to understand the geological evidence. The combination of these factors, accompanied by local

15   feedbacks can lead to strongly divergent summer temperatures in the region, which during some glacial periods could have been sufficiently low to allow for the buildup of an ice sheet, while during other glacials, above-freezing summer temperatures might have prevented a multi-year snow-pack, and hence an ice sheet, from forming. Finally, this high sensitivity of Siberian LGM summer temperatures in different climate models will present a major challenge in future modelling efforts using coupled ice-sheet-climate models.

References

Abe-Ouchi, A., Segawa, T., and Saito, F.: Climatic conditions for modelling the Northern Hemisphere ice sheets throughout the ice age cycle, Climate of the Past, 3, 423–438, https://doi.org/10.5194/cp-3-423-2007, 2007.

Abe-Ouchi, A., Saito, F., Kawamura, K., Raymo, M. E., Okuno, J., Takahashi, K., and Blatter, H.: Insolation-driven 100,000-year glacial cycles and hysteresis of ice-sheet volume, Nature, 500, 190–193, https://doi.org/10.1038/nature12374, http://dx.doi.org/10.1038/nature12374, 2013.

Adler, R. E., Polyak, L., Ortiz, J. D., Kaufman, D. S., Channell, J. E. T., Xuan, C., Grottoli, A. G., Sellén, E., and Crawford, K. A.: Sediment record from the western Arctic Ocean with an improved Late Quaternary age resolution : HOTRAX core HLY0503-8JPC , Mendeleev Ridge, Global and Planetary Change, 68, 18–29, https://doi.org/10.1016/j.gloplacha.2009.03.026, http://dx.doi.org/10.1016/j.gloplacha.2009.03.026, 2009.

Backman, J., Fornaciari, E., and Rio, D.: Marine Micropaleontology Biochronology and paleoceanography of late Pleistocene and Holocene calcareous nannofossil abundances across the Arctic Basin, Marine Micropaleontology, 72, 86–98, https://doi.org/10.1016/j.marmicro.2009.04.001, http://dx.doi.org/10.1016/j.marmicro.2009.04.001, 2009.

Basilyan, A. E., Nikolsky, P. A., Maksimov, F. E., and Kuznetsov, V. Y.: Age of Cover Glaciation of the New Siberian Islands Based on 230Th/U-dating of Mollusk Shells, Structure and Development of the Lithosphere, Paulsen, pp. 506–514, 2010.

Beghin, P., Charbit, S., Dumas, C., Kageyama, M., Roche, D. M., and Ritz, C.: Interdependence of the growth of the Northern Hemisphere ice sheets during the last glaciation: the role of atmospheric circulation, Climate of the Past, 10, 345–358, https://doi.org/10.5194/cp-10-345-2014, 2014.

Boucsein, B., Knies, J., and Stein, R.: Organic matter deposition along the Kara and Laptev Seas continental margin (eastern Arctic Ocean) during last deglaciation and Holocene : evidence from organic-geochemical and petrographical data, Marine Geology, 183, 67–87, https://www.sciencedirect.com/science/article/pii/S0025322701002493, 2002.

Braconnot, P., Otto-Bliesner, B. L., Harrison, S. P., Joussaume, S., Peterchmitt, J.-Y., Abe-Ouchi, A., Crucifix, M., Driesschaert, E., Fichefet, T., Hewitt, C. D., Kageyama, M., Kitoh, A., Laîné, A., Loutre, M.-F., Marti, O., Merkel, U., Ramstein, G., Valdes, P., Weber, S. L., Yu, Y., and Zhao, Y.: Results of PMIP2 coupled simulations of the Mid-Holocene and Last Glacial Maximum - Part 1: experiments and large-scale features, Climate of the Past, 3, 261–277, https://www.clim-past.net/3/261/2007/, 2007.

Broccoli, A. J. and Manabe, S.: The Effects of the Laurentide Ice Sheet on North American Climate during the Last Glacial Maximum, Géographie physique et Quaternaire, 41, 291–299, https://doi.org/10.7202/032684ar, http://www.erudit.org/revue/gpq/1987/v41/n2/032684ar.html, 1987.

Charbit, S., Ritz, C., Philippon, G., Peyaud, V., and Kageyama, M.: Numerical reconstructions of the Northern Hemisphere ice sheets through the last glacial-interglacial cycle, Climate of the Past, 3, https://doi.org/10.5194/cpd-2-879-2006, 2007.

Cook, K. H. and Held, I. M.: Stationary Waves of the Ice Age Climate, https://doi.org/10.1175/1520-0442(1988)001<0807:swotia>2.0.co;2, 1988.

Darby, D. A., Polyak, L., and Bauch, H. A.: Progress in Oceanography Past glacial and interglacial conditions in the Arctic Ocean and marginal seas - a review, 71, 129–144, https://doi.org/10.1016/j.pocean.2006.09.009, 2006.

Di Nezio, P. N., Timmermann, A., Tierney, J. E., Jin, F. F., Otto-Bliesner, B. L., Rosenbloom, N., Mapes, B., Neale, R. B., Ivanovic, R. F., and Montenegro, A.: The climate response of the Indo-Pacific warm pool to glacial sea level, Paleoceanography, 31, 866–894, https://doi.org/10.1002/2015PA002890, 2016.

Ehlers, J., Gibbard, P. L., and Hughes, P. D.: Quaternary Glaciations and Chronology, in: Past Glacial Environments, edited by Menzies, J. and van der Meer, J. J. M., chap. 4, Elsevier, 2018.

Ganopolski, A., Calov, R., and Claussen, M.: Simulation of the last glacial cycle with a coupled climate ice-sheet model of intermediate complexity, Climate of the Past, 6, 229–244, https://doi.org/10.5194/cp-6-229-2010, 2010.

Gualtieri, L., Vartanyan, S. L., Brigham-Grette, J., and Anderson, P. M.: Evidence for an ice-free Wrangel Island, northeast Siberia during the Last Glacial Maximum, Boreas, 34, 264–273, https://doi.org/10.1080/03009480510013097, 2005.

Harrison, S. P., Kohfeld, K. E., Roelandt, C., and Claquin, T.: The role of dust in climate changes today, at the last glacial maximum and in the future, Earth-Science Reviews, 54, 43–80, https://doi.org/10.1016/S0012-8252(01)00041-1, 2001.

Harrison, S. P., Bartlein, P. J., Izumi, K., Li, G., Annan, J. D., Hargreaves, J. C., Braconnot, P., and Kageyama, M.: Evaluation of CMIP5 palaeo-simulations to improve climate projections, Nature Climate Change, 5, 735–743, https://doi.org/10.1038/nclimate2649, http://www.nature.com/doifinder/10.1038/nclimate2649, 2015.

Hubberten, H. W., Andreev, A., Astakhov, V. I., Demidov, I., Dowdeswell, J. A., Henriksen, M., Hjort, C., Houmark-nielsen, M., Jakobsson, M., Kuzmina, S., Larsen, E., Pekka, J., Lys, A., Saarnisto, M., Schirrmeister, L., Sher, A. V., Siegert, C., Siegert, M. J., and Inge, J.: The periglacial climate and environment in northern Eurasia during the Last Glaciation, 23, 1333–1357, https://doi.org/10.1016/j.quascirev.2003.12.012, 2004.

Hurrell, J. W., Holland, M. M., Gent, P. R., Ghan, S., Kay, J. E., Kushner, P. J., Lamarque, J. F., Large, W. G., Lawrence, D. M., Lindsay, K., Lipscomb, W. H., Long, M. C., Mahowald, N. M., Marsh, D. R., Neale, R. B., Rasch, P., Vavrus, S., Vertenstein, M., Bader, D. A., Collins, W. D., Hack, J. J., Kiehl, J., and Marshall, S.: The community earth system model: A framework for collaborative research, Bulletin of the American Meteorological Society, 94, 1339–1360, https://doi.org/10.1175/BAMS-D-12-00121.1, 2013.

Ivanovic, R. F., Gregoire, L. J., Kageyama, M., Roche, D. M., Valdes, P. J., Burke, A., Drummond, R., Peltier, W. R., and Tarasov, L.: Transient climate simulations of the deglaciation 21–9 thousand years before present; PMIP4 Core experiment design and boundary conditions, Geoscientific Model Development, 9, 2563–2587, https://doi.org/10.5194/gmd-9-2563-2016, 2016.

Jahn, A., Claussen, M., Ganopolski, A., and Brovkin, V.: Quantifying the effect of vegetation dynamics on the climate of the last glacial maximum, Climate of the Past, 1, 1–7, https://doi.org/10.5194/cp-1-1-2005, 2005.

Jakobsson, M., Andreassen, K., Rún, L., Dove, D., Dowdeswell, J. A., England, J. H., Funder, S., Hogan, K., Ingólfsson, Ó., Jennings, A., Krog, N., Kirchner, N., Landvik, J. Y., Mayer, L., Mikkelsen, N., Möller, P., Niessen, F., Nilsson, J., Regan, M. O., Polyak, L., and Nørgaard-pedersen, N.: Arctic Ocean glacial history, Quaternary Science Reviews, 92, 40–67, https://doi.org/10.1016/j.quascirev.2013.07.033, http://dx.doi.org/10.1016/j.quascirev.2013.07.033, 2014.

Jakobsson, M., Nilsson, J., Anderson, L. G., Backman, J., Björk, G., Cronin, T. M., Kirchner, N., Koshurnikov, A., Mayer, L., Noormets, R., O'Regan, M., Stranne, C., Ananiev, R., Barrientos Macho, N., Cherniykh, D., Coxall, H., Eriksson, B., Flodén, T., Gemery, L., Gustafsson, Ö., Jerram, K., Johansson, C., Khortov, A., Mohammad, R., and Semiletov, I.: Evidence for an ice shelf covering the central Arctic Ocean during the penultimate glaciation, Nature Communications, 7, 1–10, https://doi.org/10.1038/ncomms10365, 2016.

Justino, F., Timmermann, A., Merkel, U., and Peltier, W. R.: An initial intercomparison of atmospheric and oceanic climatology for the ICE-5G and ICE-4G models of LGM paleotopography, Journal of Climate, 19, 3–14, https://doi.org/10.1175/JCLI3603.1, 2006.

Kageyama, M., Albani, S., Braconnot, P., Harrison, S. P., Hopcroft, P. O., Ivanovic, R. F., Lambert, F., Marti, O., Peltier, W. R., Peterschmitt, J. Y., Roche, D. M., Tarasov, L., Zhang, X., Brady, E. C., Haywood, A. M., LeGrande, A. N., Lunt, D. J., Mahowald, N. M., Mikolajewicz, U., Nisancioglu, K. H., Otto-Bliesner, B. L., Renssen, H., Tomas, R. A., Zhang, Q., Abe-Ouchi, A., Bartlein, P. J., Cao, J., Li, Q., Lohmann, G., Ohgaito, R., Shi, X., Volodin, E., Yoshida, K., Zhang, X., and Zheng, W.: The PMIP4 contribution to CMIP6 – Part 4: Sci-

entific objectives and experimental design of the PMIP4-CMIP6 Last Glacial Maximum experiments and PMIP4 sensitivity experiments, Geoscientific Model Development, 10, 4035–4055, https://doi.org/10.5194/gmd-10-4035-2017, 2017.

Kleman, J., Fastook, J., Ebert, K., Nilsson, J., and Caballero, R.: Pre-LGM northern hemisphere ice sheet topography, Climate of the Past, 9, 2365–2378, https://doi.org/10.5194/cp-9-2365-2013, 2013.

5   Krinner, G., Boucher, O., and Balkanski, Y.: Ice-free glacial northern Asia due to dust deposition on snow, Climate Dynamics, 27, 613–625, https://doi.org/10.1007/s00382-006-0159-z, 2006.

Lambert, F., Tagliabue, A., Shaffer, G., Lamy, F., Winckler, G., Farias, L., Gallardo, L., and Pol-Holz, R. D.: Dust fluxes and iron fertilization in Holocene and Last Glacial Maximum climates, Geophyscial Research Letters, pp. 6014–6023, https://doi.org/10.1002/2015GL064250.Received, https://agupubs.onlinelibrary.wiley.com/doi/full/10.1002/2015GL064250, 2015.

10   Langen, P. L. and Vinther, B. M.: Response in atmospheric circulation and sources of Greenland precipitation to glacial boundary conditions, Climate Dynamics, 32, 1035–1054, https://doi.org/10.1007/s00382-008-0438-y, 2009.

Lawrence, D. M., Oleson, K. W., Flanner, M. G., Thornton, P. E., Swenson, S. C., Lawrence, P. J., Zeng, X., Yang, Z.-L., Levis, S., Sakaguchi, K., Bonan, G. B., and Slater, A. G.: Parameterization improvements and functional and structural advances in Version 4 of the Community Land Model, Journal of Advances in Modeling Earth Systems, 3, 1–27, https://doi.org/10.1029/2011ms000045, 2011.

15   Liakka, J. and Lofverstrom, M.: Arctic warming induced by the Laurentide ice sheet topography, Climate of the Past, 14, 887–900, https://doi.org/10.5194/cp-2018-26, https://www.clim-past-discuss.net/cp-2018-26/, 2018.

Liakka, J. and Nilsson, J.: The impact of topographically forced stationary waves on local ice-sheet climate, Journal of Glaciology, 56, 534–544, https://doi.org/10.3189/002214310792447824, 2010.

Liakka, J., Colleoni, F., and Lofverstrom, M.: The impact of the North American glacial topography on the evolution of the Eurasian ice

20   sheet during the last glacial cycle, Climate of the Past, 12, 1225–1241, https://doi.org/10.5194/cp-12-1225-2016, 2016.

Mahowald, N., Kohfeld, K., Hansson, M., Balkanski, Y., Harrison, S. P., Prentice, I. C., Schulz, M., and Rodhe, H.: Dust sources and deposition during the last glacial maximum and current climate: A comparison of model results with paleodata from ice cores and marine sediments, Journal of Geophysical Research: Atmospheres, 104, 15 895–15 916, https://doi.org/10.1029/1999jd900084, 1999.

Mahowald, N. M., Yoshioka, M., Collins, W. D., Conley, A. J., Fillmore, D. W., and Coleman, D. B.: Climate response and radiative forcing

25   from mineral aerosols during the last glacial maximum, pre-industrial, current and doubled-carbon dioxide climates, Geophysical Research Letters, 33, 2–5, https://doi.org/10.1029/2006GL026126, 2006.

Meyer, V. D., Hefter, J., Lohmann, G., Max, L., Tiedemann, R., and Mollenhauer, G.: Summer temperature evolution on the Kamchatka Peninsula, Russian Far East, during the past 20000 years, Climate of the Past, 13, 359–377, https://doi.org/10.5194/cp-13-359-2017, https://www.clim-past.net/13/359/2017/cp-13-359-2017.pdf, 2017.

30   Niessen, F., Hong, J. K., Hegewald, A., Matthiessen, J., Stein, R., Kim, H., Kim, S., Jensen, L., Jokat, W., Nam, S. I., and Kang, S. H.: Repeated Pleistocene glaciation of the East Siberian continental margin, Nature Geoscience, 6, 842–846, https://doi.org/10.1038/ngeo1904, http://dx.doi.org/10.1038/ngeo1904, 2013.

Patton, H., Andreassen, K., Bjarnadóttir, L. R., Dowdeswell, J. A., Winsborrow, M. C. M., Noormets, R., Polyak, L., Auriac, A., and Hubbard, A.: Geophysical constraints on the dynamics and retreat of the Barents Sea ice sheet as a paleobenchmark for models of marine ice sheet

35   deglaciation, Reviews of Geophysics, 53, 1051–1098, https://doi.org/10.1002/2015RG000495.Received, 2015.

Peltier, W. R., Argus, D. F., and Drummond, R.: Journal of Geophysical Research : Solid Earth, Journal of Geophysical Research: Solid Earth, 2015, 450–487, https://doi.org/10.1002/2014JB011176.Received, 2015.

Pitulko, V. V., Nikolsky, P. A., Girya, E. Y., and Basilyan, A. E.: The Yana RHS Site : Humans in the Arctic before the last glacial maximum, Science, 303, https://doi.org/10.1126/science.1085219, 2004.

Polyak, L., Curry, W. B., Darby, D. A., Bischof, J., and Cronin, T. M.: Contrasting glacial / interglacial regimes in the western Arctic Ocean as exempli ¢ ed by a sedimentary record from the Mendeleev Ridge, 203, https://doi.org/10.1016/S0031-0182(03)00661-8, https://www.sciencedirect.com/science/article/pii/S0031018203006618, 2004.

Polyak, L., Darby, D. A., Bischof, J. F., and Jakobsson, M.: Stratigraphic constraints on late Pleistocene glacial erosion and deglaciation of the Chukchi margin, Arctic Ocean, Quaternary Research, 67, 234–245, https://doi.org/10.1016/j.yqres.2006.08.001, 2007.

Polyak, L., Bischof, J., Ortiz, J. D., Darby, D. A., Channell, J. E. T., Xuan, C., Kaufman, D. S., Løvlie, R., Schneider, D. A., Eberl, D. D., Adler, R. E., and Council, E. A.: Late Quaternary stratigraphy and sedimentation patterns in the western Arctic Ocean, Global and Planetary Change, 68, 5–17, https://doi.org/10.1016/j.gloplacha.2009.03.014, http://dx.doi.org/10.1016/j.gloplacha.2009.03.014, 2009.

Roe, G. H. and Lindzen, R. S.: A one-dimensional model for the interaction between continental-scale ice sheets and atmospheric stationary waves, Climate Dynamics, 17, 479–487, https://doi.org/10.1007/s003820000123, http://link.springer.com/10.1007/s003820000123, 2001.

Sanberg, J. A. M. and Oerlemans, J.: Modelling of Pleistocene European ice sheets: the effect of upslope precipitation, Geologie en Mijn-bouw, 1983.

Schenk, F., Väliranta, M., Muschitiello, F., Tarasov, L., Heikkilä, M., Björck, S., Brandefelt, J., Johansson, A. V., Näslund, J., and Wohlfarth, B.: Warm summers during the Younger Dryas cold reversal, Nature Communications, 9, 1634, https://doi.org/10.1038/s41467-018-04071-5, http://www.nature.com/articles/s41467-018-04071-5, 2018.

Schirrmeister, L.: [230]Th/U Dating of Frozen Peat , Bol'shoy Lyakhovsky Island (Northern Siberia), 258, 253–258, https://doi.org/10.1006/qres.2001.2306, 2002.

Stauch, G. and Gualtieri, L.: Late Quaternary glaciations in northeastern Russia, 23, 545–558, https://doi.org/10.1002/jqs, 2008.

Svendsen, J. I., Alexanderson, H., Astakhov, V. I., Demidov, I., Dowdeswell, J. A., Funder, S., Gataullin, V., Henriksen, M., Hjort, C., Houmark-Nielsen, M., Hubberten, H. W., Ingólfsson, Ó., Jakobsson, M., Kjær, K. H., Larsen, E., Lokrantz, H., Lunkka, J. P., Lyså, A., Mangerud, J., Matiouchkov, A., Murray, A., Möller, P., Niessen, F., Nikolskaya, O., Polyak, L., Saarnisto, M., Siegert, C., Siegert, M. J., Spielhagen, R. F., and Stein, R.: Late Quaternary ice sheet history of northern Eurasia, Quaternary Science Reviews, 23, 1229–1271, https://doi.org/10.1016/j.quascirev.2003.12.008, https://www.sciencedirect.com/science/article/pii/S0277379103003421, 2004.

Ullman, D. J., Legrande, A. N., Carlson, A. E., Anslow, F. S., and Licciardi, J. M.: Assessing the impact of laurentide ice sheet topography on glacial climate, Climate of the Past, 10, 487–507, https://doi.org/10.5194/cp-10-487-2014, 2014.

Wetterich, S., Rudaya, N., Tumskoy, V., Andreev, A. A., Opel, T., Schirrmeister, L., and Meyer, H.: Last Glacial Maximum records in permafrost of the East Siberian Arctic, Quaternary Science Reviews, 30, 3139–3151, https://doi.org/10.1016/j.quascirev.2011.07.020, http://dx.doi.org/10.1016/j.quascirev.2011.07.020, 2011.

Willeit, M. and Ganopolski, A.: The importance of snow albedo for ice sheet evolution over the last glacial cycle, Climate of the Past, 14, 697–707, https://doi.org/10.5194/cp-14-697-2018, 2018.

Yanase, W. and Abe-Ouchi, A.: The LGM surface climate and atmospheric circulation over East Asia and the North Pacific in the PMIP2 coupled model simulations, Climate of the Past, 3, 439–451, https://doi.org/10.5194/cp-3-439-2007, 2007.

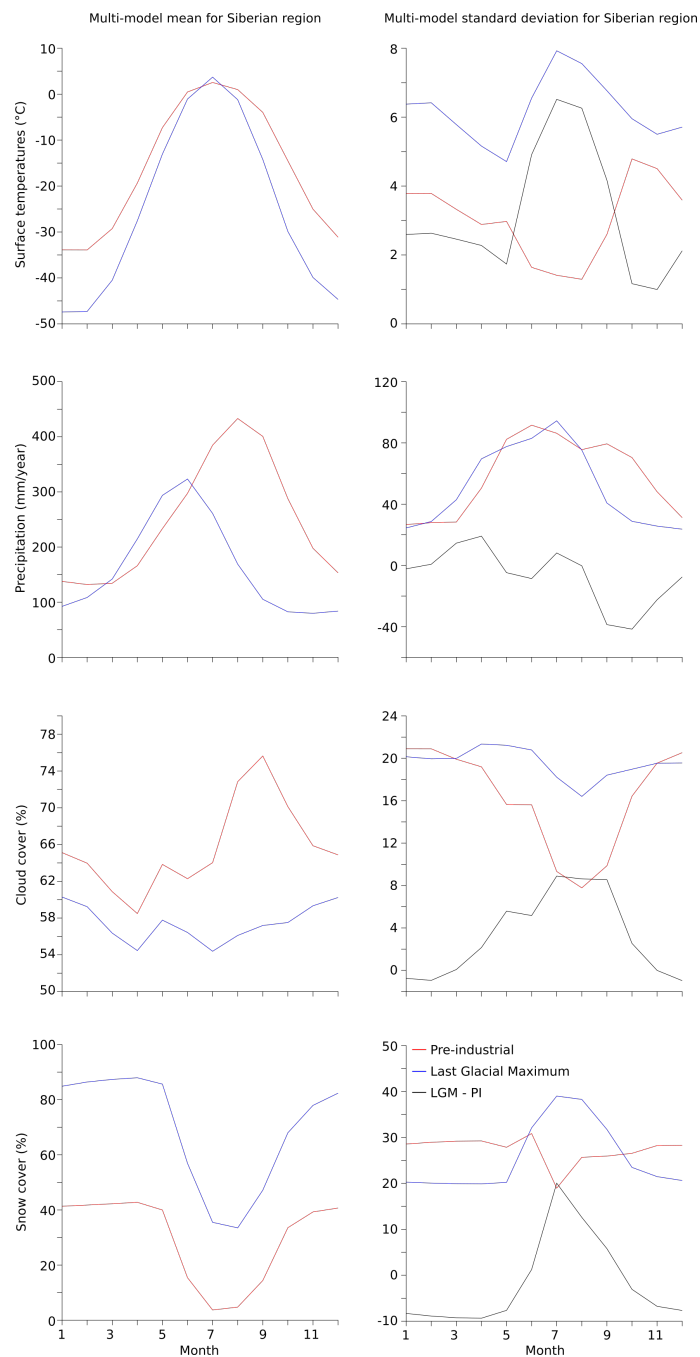**Figure A1.** PMIP2 and PMIP3 multi-model mean (left panels) and multi-model standard deviation (right panels) seasonal cycles of selected variables for PI (red), LGM (blue) and LGM anomalies (LGM - PI; black). Mean and standard deviation calculated for the Siberian target region. Top row: temperatures ($^{\circ}$C); Second row: precipitation (mmyr^{-1}); Third row: cloud cover (%); Bottom row: snow cover (%).

Table 1. List with PMIP2 and PMIP3 climate models included in the analysis with details on grid resolution and usage of interactive vegetation. <mark>In the last column the simulated LGM JJA surface temperature anomaly (K) in the Siberian target region with respect to the pre-industrial is given for reference.</mark> The following abbreviations are used: Atm (atmospheric grid resolution), Ocn (ocean grid resolution), L (number of levels in the vertical). See https://pmip2.lsce.ipsl.fr and https://pmip3.lsce.ipsl.fr for further details and references.

Model	Institution	Grid Resolution	Interactive vegetation	PMIP phase	ΔT
CCSM3	National Center for Atmospheric Research, USA	Atm: 128 x 64 x L26 Ocn: 320 x 384 x L40	No	2	-3.02
CNRM-CM3.3	Centre National de Recherches Meteorologiques, France	Atm: 256 x 128 x L31 Ocn: 362 x 292 x L42	No	2	12.39
ECHAM5-MPIOM	Max Planck Institute for Meteorology, Germany	Atm: 96 x 48 x L19 Ocn: 120 x 101 x L40	Yes	2	-5.84
FGOALS1.0_g	LASG/Institute of Atmospheric Physics, China	Atm: 128 x 60 x L26 Ocn: 360 x 180 x L33	No	2	-12.13
HadCM3_AO	UK Met Office Hadley Centre, UK	Atm: 96 x 72 x L19 Ocn: 288 x 144 x L20	No	2	3.18
HadCM3_AOV	UK Met Office Hadley Centre, UK	Atm: 96 x 72 x L19 Ocn: 288 x 144 x L20	Yes	2	2.44
IPSL-CM4_v1	Institut Pierre Simon Laplace, France	Atm: 96 x 72 x L19 Ocn: 182 x 149 x L31	No	2	-0.81
MIROC3.2.2	Center for Climate System Research, JAMSTEC, Japan	Atm: 128 x 64 x L20 Ocn: 256 x 192 x L43	No	2	-1.90
CCSM4	National Center for Atmospheric Research, USA	Atm: 288 x 192 x L26 Ocn: 320 x 384 x L60	Yes	3	-7.01
CNRM-CM5	CNRM - C. Européen de Rech. Formation Avancée Calcul Sci.	Atm: 256 x 128 x L31 Ocn: 362 x 292 x L42	No	3	13.22
COSMOS-ASO	Max Planck Institute for Meteorology, Germany	Atm: 96 x 48 x L19 Ocn: 120 x 101 x L40	Yes	3	-2.41
FGOALS_g2	ASG/Institute of Atmospheric Physics, China	Atm: 128 x 60 x L26 Ocn: 360 x 180 x L30	No	3	-10.01
GISS-E2-R	NASA Goddard Institute for Space Studies	Atm: 144 x 90 x L40 Ocn: 288 x 180 x L32	No	3	-12.43
IPSL-CM5A-LR	Institut Pierre Simon Laplace, France	Atm: 96 x 96 x L39 Ocn: 182 x 149 x L31	Yes	3	3.35
MIROC-ESM	Center for Climate System Research, JAMSTEC, Japan	Atm: 128 x 64 x L80 Ocn: 256 x 192 x L44	Yes	3	1.91
MPI-ESM-P	Max Planck Institute for Meteorology, Germany	Atm: 196 x 98 x L47 Ocn: 256 x 220 x L40	Yes	3	3.35
MRI-CGCM3	Meteorological Research Institute (MRI)	Atm: 320 x 160 x L48 Ocn: 364 x 368 x L51	No	3	1.14

Table 2. List of simulations included in the three sets of CESM LGM experiments and the PI reference simulations. The following abbreviations are used: noVeg = No interactive vegetation; Veg = Including interactive vegetation; PI = pre-industrial; LGM = Last Glacial Maximum; CAM4/5 = Community Atmosphere Model version 4 or version 5; GLAC-1D = GLAC-1D ice sheet reconstruction (Ivanovic et al., 2016); ice6g = ICE-6G ice sheet reconstruction (Peltier et al., 2015).

Experiment set	Experiment name	Atmospheric model	Interactive vegetation	Boundary conditions	LGM ice-sheet reconstruction
PI reference simulations	PI_CAM4_noVeg	CAM4	No	PI	
	PI_CAM5_noVeg	CAM5	No	PI	
	PI_CAM4_Veg	CAM4	Yes	PI	
	PI_CAM5_Veg	CAM5	Yes	PI	
Continental ice sheets	LGM_CAM5_noVeg	CAM5	No	LGM	GLAC-1D
	LGM_CAM5_noVeg_ice6g	CAM5	No	LGM	ICE-6G
Atmospheric model physics	LGM_CAM4_noVeg	CAM4	No	LGM	GLAC-1D
	LGM_CAM5_noVeg	CAM5	No	LGM	GLAC-1D
Interactive vegetation	LGM_CAM4_noVeg	CAM4	No	LGM	GLAC-1D
	LGM_CAM4_Veg	CAM4	Yes	LGM	GLAC-1D
	LGM_CAM5_noVeg	CAM5	No	LGM	GLAC-1D
	LGM_CAM5_Veg	CAM5	Yes	LGM	GLAC-1D

Table 3. Simulated CESM PI and LGM climatic conditions in the Siberian target region. For the abbreviations see table 2. Note that LGM JJA sea level pressure show here have been corrected for LGM to PI differences in global mean sea level pressure.

	Experiment name	JJA temperatures °C	JJA precipitation mm month^{-1}	JJA cloud cover %	JJA sea level pressure hPa	Minimum snow cover %	JJA snow cover %
PI reference simulations	PI_CAM4_noVeg	7.96	5.54	55.07	1009	1.27	10.92
	PI_CAM5_noVeg	10.72	3.12	65.74	1012	0.04	1.65
	PI_CAM4_Veg	6.52	6.70	54.20	1009	2.84	23.08
	PI_CAM5_Veg	8.35	6.47	62.39	1013	0.35	13.88
LGM simulations	LGM_CAM4_noVeg	8.47	4.22	45.42	1010	0.58	5.79
	LGM_CAM5_noVeg	9.02	7.44	62.59	1011	0.58	4.53
	LGM_CAM4_Veg	1.40	10.54	46.84	1011	16.75	43.73
	LGM_CAM5_Veg	-12.06	20.28	70.43	1019	100.00	100.00
	LGM_CAM5_noVeg_ice6g	5.97	11.42	58.19	1013	2.46	9.56